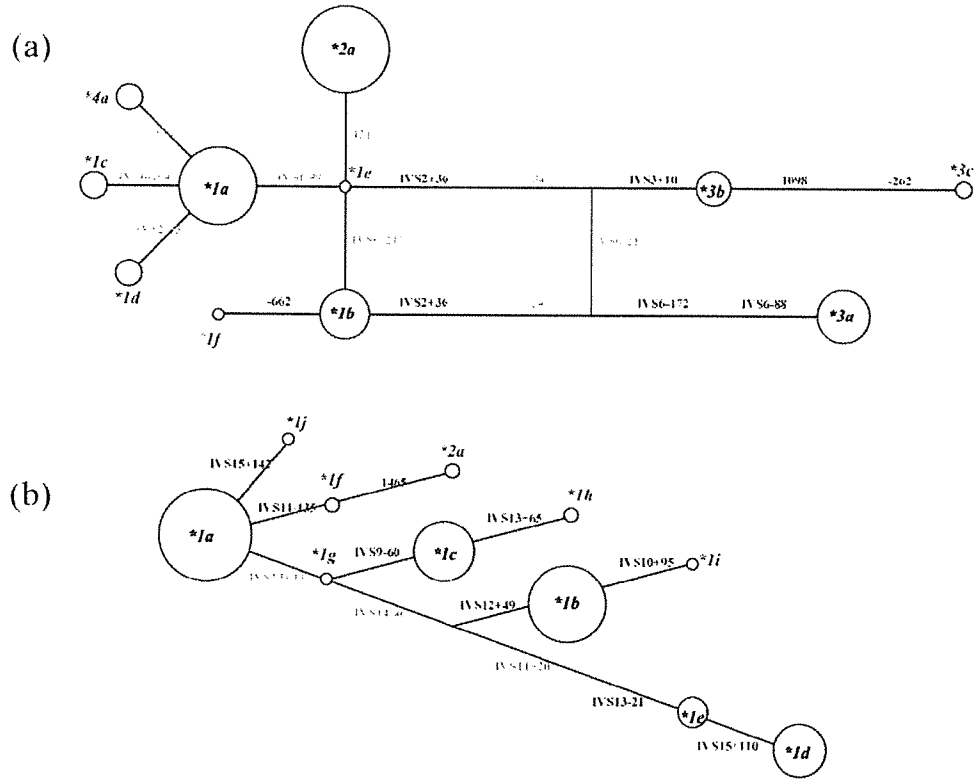

Fig. 3. Network analysis of *ABCG2* haplotypes of Block 1 (a) and Block 2 (b). Haplotypes found in at least two patients are shown. The areas in the circles represent the approximate frequencies of each haplotype. The variations connecting adjacent haplotypes are indicated using their positions. The htSNPs are indicated in red.

which were in strong LD ($r^2 = 0.709$) as described above. Our block partitioning was compatible with the definition of the LD block:[33] 254 pairs (92%) out of all 276 pairs in Block 1 and 127 pairs (93%) out of all 136 pairs in Block 2 gave pair-wise $|D'|$ values greater than 0.9.

Haplotype estimation, selection of htSNPs and network analysis: First, diplotypes/haplotypes within each *ABCG2* block were inferred. Using all 2, 24, and 17 variations in Block −1, Block 1, and Block 2, respectively, 3 (Block −1), 23 (Block 1), and 17 (Block 2) haplotypes were inferred (**Tables 3–5**). The probabilities of diplotype configurations in Block −1, Block 1, and Block 2 were over 0.95 for 100%, 97.7%, and 97.2% of the subjects, respectively. Of all the estimated haplotypes (except for the unambiguously identified haplotypes), 1 in Block −1, 10 in Block 1, and 4 in Block 2 were inferred in only one patient. Since the estimation of rare haplotypes is often ambiguous, they were classified into "Others" within each group (the **1* and **3* groups in Block 1) or indicated with a "?".

In Block −1, three haplotype (**1a*, **1b*, and **1c*) were inferred. The frequencies of the common haplotypes, **1a* and **1b*, were 0.763 and 0.234, respectively.

In Block 1, seven haplotype groups (**1* to **7*) were inferred, and the groups of **2* to **7* harbored nonsynonymous SNPs, 421C>A (Gln141Lys) (**2*), 34G>A (Val12Met) (**3*), 376C>T (Gln126X) (**4*), 38C>T (Ser13Leu) (**5*), 479G>A (Arg160Gln) (**6*), and 1060G>A (Gly354Arg) (**7*). The most dominant haplotype was **2a* (0.319 frequency), followed by **1a* (0.260), **3a* (0.121), **1b* (0.105), **3b* (0.051), **1c* (0.031), **1d* (0.028), and **4a* (0.028). These 8 common haplotypes, found in 10 or more patients, accounted for 94% of all the inferred haplotypes. The nonsynonymous **5* to **7* groups were rare and found at frequencies less than 0.003. The haplotype-tagging SNPs (htSNPs) that were able to resolve the 8 common haplotypes were the following 7 variations: IVS1-99G>A, 34G>A (Val12Met), IVS2-93T>C, 376C>T (Gln126X), 421C>A (Gln141Lys), IVS6-217A>G, and IVS6-204C>T. The result of Network analysis in Block 1 is shown in **Fig. 3a**. The cladogram shows that **1a* and its closely connected haplotypes (**1c*, **1d*, and **4a*) are distant from the **3* group.

In Block 2, five haplotype groups (**1* to **5*) were inferred. The groups of **2* to **5* were defined as the

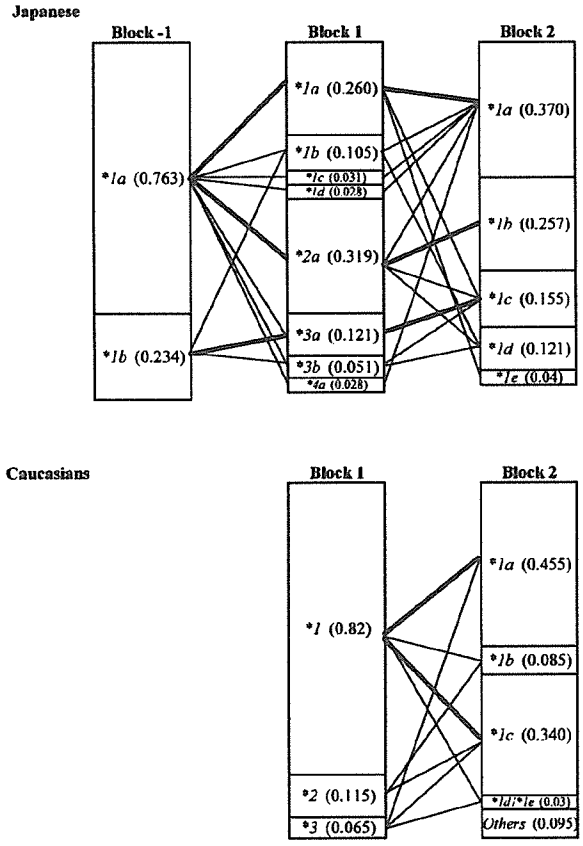

Fig. 4. The combination profiles of block haplotypes in Japanese (upper panel) and in Caucasians (lower panel) are shown. The haplotypes in Caucasians were classified based on our criteria from the previous report by Bosch *et al.*[7] The haplotypes in Block −1 were not available in Caucasians. The thick lines represent the combinations with frequencies over 10%, and the thin lines represent the combinations with frequencies of 1.0 to 9.9%.

haplotype harboring nonsynonymous SNPs, 1465T>C (Phe489Leu) (**2*), 1291T>C (Phe431Leu) (**3*), 1322G>A (Ser441Asn)/1515delC (Phe506SerfsX) (**4*), and 1723C>T (Arg575X) (**5*), respectively. Of them, **3a*, **4a*, and **5a* were inferred in only one patient, and the assignment of concurring SNPs was ambiguous. Five common haplotypes found in 10 or more patients (**1a*-**1e*) account for 94% of all the observed haplotypes. We found that 3 htSNPs, IVS11+20A>G, IVS13+40C>T, and IVS14-46A>G, are sufficient to distinguish four major haplotypes (**1a*-**1d*), which account for 90% of all the inferred haplotypes. The cladogram of network analysis suggests that the most common haplotype, **1a*, is the root of the tree (**Fig. 3b**).

Next, the combinations of block haplotypes were analyzed (inter-block haplotypes, **Fig. 4**). Between Blocks −1 and 1, both **1a* and **2a* in Block 1 were completely linked with Block −1 **1a*. In contrast, **3a* in Block 1 was mostly linked with Block −1 **1b*. As for combinations between Blocks 1 and 2, **1a*, **2a*, and **3a* in Block 1 were mostly linked with Block 2 **1a*, **1b*, and **1c*, respectively. Among the three blocks, the following combinations were major: Block −1 **1a*-Block 1 **2a*-Block 2 **1b* (0.246 frequency), Block −1 **1a*-Block 1 **1a*-Block 2 **1a* (0.192), and Block −1 **1b*-Block 1 **3a*-Block 2 **1c* (0.088).

Discussion

The present study provides comprehensive data on genetic variation in *ABCG2*, a gene encoding a multidrug transporter that is involved in the efficacy of cancer chemotherapy. Eleven nonsynonymous variations, including two novel ones (Ser13Leu and Gly354Arg), were found.

As for three of the reported nonsynonymous SNPs, *in vitro* functional analysis has already been performed to identify their effects on the localization, expression levels, and transport activity. Mizuarai *et al.* showed that 34G>A (Val12Met) was associated with reduced drug resistance in polarized LLC-PK1 cells, which might be caused by its impaired apical membrane localization.[25] In contrast, several groups did not find any significant effects of Val12Met on the protein expression levels as well as drug resistance using stable and transient mammalian expression systems.[16,24,26] According to Imai *et al.* and Kondo *et al.*,[16,24] the Gln141Lys substitution resulted in decreased protein expression and reduced drug resistance. These results are inconsistent with those obtained by Mizuarai *et al.* and Morisaki *et al.*, in which the reduced drug resistance was not caused by the decreased protein expression.[25,26] Kondo *et al.* have shown that the Ser441Asn variant was not localized to apical membranes, but remains intracellular in the transfected LLC-PK1 cells,[24] suggesting its reduced activity. Three variations, Gln126X, Phe506SerfsX4, and Arg575X, result in truncated proteins. Although there is limited information about the structural elements of ABCG2 responsible for its substrate recognition and transporting activity,[34] they are likely to lead to functional defects.

The functional effects of the other five nonsynonymous SNPs (Ser13Leu, Arg160Gln, Gly354Arg, Phe431Leu, and Phe489Leu) have not yet been characterized. Using the PolyPhen program (http://www.bork.embl-heidelberg.de/PolyPhen/) to predict the functional effect of these amino acid substitutions, three substitutions, Ser13Leu, Arg160Gln, and Gly354Arg, were estimated to cause possible alterations in protein function based on the PSIC (position specific independent count) profile score. Notably, Arg160Gln is located in the functionally important ATP-binding region between the Waker A (amino acids 80-89) and Walker B (amino acids 206-210) motifs. Thus, func-

tional analysis of these variants is warranted. Except for Val12Met, Gln126X, and Gln141Lys, the allele frequencies of eight nonsynonymous SNPs were less than 0.01, and these low frequency variations do not largely contribute to the overall heterozygosity of *ABCG2*; however, they might have clinical importance.

Bailey-Dell *et al.* characterized the basal promoter of *ABCG2*, which was mapped in the region from −859 to −187 relative to the translational initiation site and contained a CCAAT box and multiple Sp1 sites.[30] Two novel SNPs in the 5′ flanking region, −753T>C and −662C>T, are located near the putative SP1 binding site in the basal promoter. However, the functional significance of these SNPs is currently unknown.

It has been well recognized that partitioning of haplotype blocks and selection of their htSNPs are useful for association studies.[35] The resulting limited haplotype diversity would offer statistically sufficient power to detect phenotypic differences. In fact, due to the intragenic recombinations in *ABCG2*, too many whole-gene haplotypes (57 haplotypes), each having low frequencies, were inferred with low probabilities when all the 43 detected variations were used (data not shown). Since the LD analysis of *ABCG2* in the Japanese revealed at least two recombination sites, three LD blocks were assigned, which led to the identification of several htSNPs that could discriminate common haplotypes. Our analysis was focused on cancer patients in this study, but the allele frequencies obtained for the common polymorphisms were comparable to those in previous reports[16,23] and the JSNPs database. Thus, the population in this study is likely to represent the general Japanese population. Therefore, we compared our results on the LD patterns and haplotype distribution in Japanese with those in a closely related population (Chinese) and in a distant population (Caucasian).

The LD profile and haplotype structure of *ABCG2* in Chinese was reported recently by Wang *et al.*[20] The LD profile was similar between Japanese and Chinese. Because they did not use the eight common variations detected in our study (−1203 −1200delCTCA, IVS1-99G>A, IVS6-217A>G, IVS6-204C>T, IVS6-172A>G, IVS6-88A>G, IVS9-60A>T, and IVS15+110C>T), their haplotypes do not exactly correspond to ours. Nevertheless, the frequency (31.9%) of the haplotype **2a* in Block 1 harboring 421C>A (Gln141Lys) was comparable to their counterpart (20.4%). In both their (Chinese) and our (Japanese) studies, neither *cis*-acting regulatory polymorphisms nor other common nonsynonymous SNPs in the haplotype **2a* have been detected. Therefore, the substitution itself of Gln141 to Lys is likely to be responsible for the reduced expression of ABCG2 protein in placenta as demonstrated by Kobayashi *et al.*[23] Furthermore, Chinese and Japanese share several common Block 2 haplotypes, **1a*, **1b*, **1c*, and **1d*/**1e*. The frequencies of these haplotypes in Japanese were comparable to those in Chinese (0.222, 0.204, 0.259, and 0.222, respectively).[20]

Recently, the *ABCG2* haplotypes in Caucasians have been reported by Bosch *et al.*[21] by using 19 SNPs detected in a Dutch population. Since their haplotype analysis was conducted using the whole *ABCG2* gene (from exons 2 to 16) as one block, we compared our results with theirs in terms of our Block 1 and Block 2 haplotypes. The haplotype distribution in Caucasians is different from that in Japanese (**Fig. 4**). In Block 1, the frequencies of **2a* (0.115), **3a* (0.05), and **3b* (0.015) in Caucasians are much lower than those in Japanese (0.319, 0.121, and 0.051, respectively). In contrast, the **1* group in Caucasians is much more frequent (0.82) than those in Japanese (0.45). We could not compare the frequencies of the **1* subtypes because the 5 common SNPs detected in our study (IVS1-99G>A, IVS6-217A>G, IVS6-204C>T, IVS6-172A>G, and IVS6-88A>G) were not genotyped in these subjects. In Block 2, the frequencies of **1a* were comparable between Japanese (0.370) and Caucasians (0.455). However, **1b* and **1c* in Caucasians was observed with much lower (0.085) and higher (0.34) frequencies, respectively, than those in Japanese (0.257 and 0.155). Our results suggest that the optimal sets of the htSNPs for *ABCG2* differ to some extent between ethnic groups although the common SNPs are shared between them.

Despite the past recombinations within *ABCG2*, three major inter-block haplotypes were relatively well conserved in Japanese: Block −1 **1a*-Block 1 **2a*-Block 2 **1b* (0.246 frequency), Block −1 **1a*-Block 1 **1a*-Block 2 **1a* (0.192), and Block −1 **1b*-Block 1 **3a*-Block 2 **1c* (0.088). Because the variation, −1203 −1200delCTCA in Block −1 was not screened in both Chinese[20] and Dutch populations[21], we could not assess the associations between Block −1 and Block 1 SNPs in these ethnic groups. In a Swedish population, −1203 −1200delCTCA was reported to be linked with 34G>A (Val12Met), the representative SNP in the Block1 **3* group.[19] Due to the high (0.54) and low (0.02) allele frequencies of −1203 −1200delCTCA and 34G>A (Val12Met), respectively, the Block −1 **1b*-Block 1 **3* combination is not predominant in the Swedish population. Zhou *et al.* suggested that −1203 −1200delCTCA might influence pharmacokinetic parameters of irinotecan.[31] On the other hand, the functional significance of 34G>A (Val12Met) is not fully elucidated as described above.[16,24,26] In this context, the major combination in Japanese, Block −1 **1b*-Block 1 **3a*, should be carefully considered in pharmacogenetic studies in Japanese. As for the combinations of haplotypes between Blocks 1 and 2, Block 1 **2a*-Block 2 **1b*, was observed in Chinese[20] and

Caucasians[21] with frequencies of 0.204 and 0.05, respectively, as well as in Japanese (0.246 frequency). In contrast, Block 1 **3a*-Block 2 **1c* is characteristic of the Japanese. Because Block 2 **1c* was mostly connected to the **1* group in Block 1 in Caucasians,[21] the frequency of Block1 ***1**-Block 2 **1c* was higher in Caucasians (0.29) than in Japanese (0.02), while the frequency of Block 1 **3a*-Block 2 **1c* was lower in Caucasians (0.02) than in Japanese (0.102). The profiles of recombinations in *ABCG2* seem to vary among ethnic groups, although the direct comparisons of LD patterns using the same SNPs between Japanese and other major ethnicities are needed to address this issue.

In conclusion, 43 variations were identified in *ABCG2*, including 11 novel ones, in a Japanese population. Two novel SNPs resulted in amino acid substitutions. Based on the LD profile and haplotypes of *ABCG2*, several htSNPs were found that are sufficient to distinguish the major *ABCG2* haplotypes in Japanese. This is the first report on *ABCG2* haplotypes with high-density SNPs in Japanese. This information will be useful in pharmacogenetic studies that investigate the relationship between interindividual differences of drug disposition and *ABCG2* haplotypes.

Acknowledgments: We thank Ms. Chie Sudo for her secretarial assistance.
This study was supported in part by the Program for the Promotion of Fundamental Studies in Health Sciences and in part by the Health and Labor Sciences Research Grants from the Ministry of Health, Labor and Welfare.

References

1) Miyake, K., Mickley, L., Litman, T., Zhan, Z., Robey, R., Cristensen, B., Brangi, M., Greenberger, L., Dean, M., Fojo, T. and Bates, S. E.: Molecular cloning of cDNAs which are highly overexpressed in mitoxantrone-resistant cells: demonstration of homology to ABC transport genes. *Cancer Res.*, **59**: 8-13 (1999).
2) Doyle, L. A., Yang, W., Abruzzo, L. V., Krogmann, T., Gao, Y., Rishi, A. K. and Ross, D. D.: A multidrug resistance transporter from human MCF-7 breast cancer cells. *Proc. Natl. Acad. Sci. U S A*, **95**: 15665-15670 (1998).
3) Allikmets, R., Schriml, L. M., Hutchinson, A., Romano-Spica, V. and Dean, M.: A human placenta-specific ATP-binding cassette gene (ABCP) on chromosome 4q22 that is involved in multidrug resistance. *Cancer Res.*, **58**: 5337-5339 (1998).
4) Allen, J. D., Brinkhuis, R. F., Wijnholds, J. and Schinkel, A. H.: The mouse Bcrp1/Mxr/Abcp gene: amplification and overexpression in cell lines selected for resistance to topotecan, mitoxantrone, or doxorubicin. *Cancer Res.*, **59**: 4237-4241 (1999).
5) Kage, K., Tsukahara, S., Sugiyama, T., Asada, S., Ishikawa, E., Tsuruo, T. and Sugimoto, Y.: Dominant-negative inhibition of breast cancer resistance protein as drug efflux pump through the inhibition of S-S dependent homodimerization. *Int. J. Cancer*, **97**: 626-630 (2002).
6) Xu, J., Liu, Y., Yang, Y., Bates, S. and Zhang, J. T.: Characterization of oligomeric human half-ABC transporter ATP-binding cassette G2. *J. Biol. Chem.*, **279**: 19781-19789 (2004).
7) Maliepaard, M., Scheffer, G. L., Faneyte, I. F., van Gastelen, M. A., Pijnenborg, A. C., Schinkel, A. H., van De Vijver, M. J., Scheper, R. J. and Schellens, J. H.: Subcellular localization and distribution of the breast cancer resistance protein transporter in normal human tissues. *Cancer Res.*, **61**: 3458-3464 (2001).
8) Maliepaard, M., van Gastelen, M. A., de Jong, L. A., Pluim, D., van Waardenburg, R. C., Ruevekamp-Helmers, M. C., Floot, B. G. and Schellens, J. H.: Overexpression of the BCRP/MXR/ABCP gene in a topotecan-selected ovarian tumor cell line. *Cancer Res.*, **59**: 4559-4563 (1999).
9) Kawabata, S., Oka, M., Shiozawa, K., Tsukamoto, K., Nakatomi, K., Soda, H., Fukuda, M., Ikegami, Y., Sugahara, K., Yamada, Y., Kamihira, S., Doyle, L. A., Ross, D. D. and Kohno, S.: Breast cancer resistance protein directly confers SN-38 resistance of lung cancer cells. *Biochem. Biophys. Res. Commun.*, **280**: 1216-1223 (2001).
10) Nakatomi, K., Yoshikawa, M., Oka, M., Ikegami, Y., Hayasaka, S., Sano, K., Shiozawa, K., Kawabata, S., Soda, H., Ishikawa, T., Tanabe, S. and Kohno, S.: Transport of 7-ethyl-10-hydroxycamptothecin (SN-38) by breast cancer resistance protein ABCG2 in human lung cancer cells. *Biochem. Biophys. Res. Commun.*, **288**: 827-832 (2001).
11) Jonker, J. W., Smit, J. W., Brinkhuis, R. F., Maliepaard, M., Beijnen, J. H., Schellens, J. H. and Schinkel, A. H.: Role of breast cancer resistance protein in the bioavailability and fetal penetration of topotecan. *J. Natl. Cancer Inst.*, **92**: 1651-1656 (2000).
12) Kruijtzer, C. M., Beijnen, J. H., Rosing, H., ten Bokkel Huinink, W. W., Schot, M., Jewell, R. C., Paul, E. M. and Schellens, J. H.: Increased oral bioavailability of topotecan in combination with the breast cancer resistance protein and P-glycoprotein inhibitor GF120918. *J. Clin. Oncol.*, **20**: 2943-2950 (2002).
13) Honjo, Y., Hrycyna, C. A., Yan, Q. W., Medina-Perez, W. Y., Robey, R. W., van de Laar, A., Litman, T., Dean, M. and Bates, S. E.: Acquired mutations in the MXR/BCRP/ABCP gene alter substrate specificity in MXR/BCRP/ABCP-overexpressing cells. *Cancer Res.*, **61**: 6635-6639 (2001).
14) Honjo, Y., Morisaki, K., Huff, L. M., Robey, R. W., Hung, J., Dean, M. and Bates, S. E.: Single-nucleotide polymorphism (SNP) analysis in the ABC half-transporter ABCG2 (MXR/BCRP/ABCP1). *Cancer Biol. Ther.*, **1**: 696-702 (2002).
15) Iida, A., Saito, S., Sekine, A., Mishima, C., Kitamura, Y., Kondo, K., Harigae, S., Osawa, S. and Nakamura, Y.: Catalog of 605 single-nucleotide polymorphisms (SNPs) among 13 genes encoding human ATP-binding

cassette transporters: ABCA4, ABCA7, ABCA8, ABCD1, ABCD3, ABCD4, ABCE1, ABCF1, ABCG1, ABCG2, ABCG4, ABCG5, and ABCG8. *J. Hum. Genet.*, **47**: 285-310 (2002).

16) Imai, Y., Nakane, M., Kage, K., Tsukahara, S., Ishikawa, E., Tsuruo, T., Miki, Y. and Sugimoto, Y.: C421A polymorphism in the human breast cancer resistance protein gene is associated with low expression of Q141K protein and low-level drug resistance. *Mol. Cancer Ther.*, **1**: 611-616 (2002).

17) Itoda, M., Saito, Y., Shirao, K., Minami, H., Ohtsu, A., Yoshida, T., Saijo, N., Suzuki, H., Sugiyama, Y., Ozawa, S. and Sawada, J.: Eight novel single nucleotide polymorphisms in ABCG2/BCRP in Japanese cancer patients administered irinotacan. *Drug Metab. Pharmacokinet.*, **18**: 212-217 (2003).

18) Zamber, C. P., Lamba, J. K., Yasuda, K., Farnum, J., Thummel, K., Schuetz, J. D. and Schuetz, E. G.: Natural allelic variants of breast cancer resistance protein (BCRP) and their relationship to BCRP expression in human intestine. *Pharmacogenetics*, **13**: 19-28 (2003).

19) Backstrom, G., Taipalensuu, J., Melhus, H., Brandstrom, H., Svensson, A. C., Artursson, P. and Kindmark, A.: Genetic variation in the ATP-binding cassette transporter gene ABCG2 (BCRP) in a Swedish population. *Eur. J. Pharm. Sci.*, **18**: 359-364 (2003).

20) Wang, H., Hao, B., Zhou, K., Chen, X., Wu, S., Zhou, G., Zhu, Y. and He, F.: Linkage disequilibrium and haplotype architecture for two ABC transporter genes (ABCC1 and ABCG2) in Chinese population: implications for pharmacogenomic association studies. *Ann. Hum. Genet.*, **68**: 563-573 (2004).

21) Bosch, T. M., Kjellberg, L. M., Bouwers, A., Koeleman, B. P., Schellens, J. H., Beijnen, J. H., Smits, P. H. and Meijerman, I.: Detection of single nucleotide polymorphisms in the ABCG2 gene in a Dutch population. *Am. J. Pharmacogenomics*, **5**: 123-131 (2005).

22) Zamboni, W. C., Bowman, L. C., Tan, M., Santana, V. M., Houghton, P. J., Meyer, W. H., Pratt, C. B., Heideman, R. L., Gajjar, A. J., Pappo, A. S. and Stewart, C. F.: Interpatient variability in bioavailability of the intravenous formulation of topotecan given orally to children with recurrent solid tumors. *Cancer Chemother Pharmacol.*, **43**: 454-460 (1999).

23) Kobayashi, D., Ieiri, I., Hirota, T., Takane, H., Maegawa, S., Kigawa, J., Suzuki, H., Nanba, E., Oshimura, M., Terakawa, N., Otsubo, K., Mine, K. and Sugiyama, Y.: Functional assessment of ABCG2 (BCRP) gene polymorphisms to protein expression in human placenta. *Drug Metab. Dispos.*, **33**: 94-101 (2005).

24) Kondo, C., Suzuki, H., Itoda, M., Ozawa, S., Sawada, J., Kobayashi, D., Ieiri, I., Mine, K., Ohtsubo, K. and Sugiyama, Y.: Functional analysis of SNPs variants of BCRP/ABCG2. *Pharm. Res.*, **21**: 1895-1903 (2004).

25) Mizuarai, S., Aozasa, N. and Kotani, H.: Single nucleotide polymorphisms result in impaired membrane localization and reduced ATPase activity in multidrug transporter ABCG2. *Int. J. Cancer.*, **109**: 238-246 (2004).

26) Morisaki, K., Robey, R. W., Ozvegy-Laczka, C., Honjo, Y., Polgar, O., Steadman, K., Sarkadi, B. and Bates, S. E.: Single nucleotide polymorphisms modify the transporter activity of ABCG2. *Cancer Chemother. Pharmacol.*, **56**: 161-172 (2005).

27) de Jong, F. A., Marsh, S., Mathijssen, R. H., King, C., Verweij, J., Sparreboom, A. and McLeod, H. L.: ABCG2 pharmacogenetics: ethnic differences in allele frequency and assessment of influence on irinotecan disposition. *Clin. Cancer Res.*, **10**: 5889-5894 (2004).

28) Sparreboom, A., Gelderblom, H., Marsh, S., Ahluwalia, R., Obach, R., Principe, P., Twelves, C., Verweij, J. and McLeod, H. L.: Diflomotecan pharmacokinetics in relation to ABCG2 421C>A genotype. *Clin. Pharmacol. Ther.*, **76**: 38-44 (2004).

29) Kitamura, Y., Moriguchi, M., Kaneko, H., Morisaki, H., Morisaki, T., Toyama, K. and Kamatani, N.: Determination of probability distribution of diplotype configuration (diplotype distribution) for each subject from genotypic data using the EM algorithm. *Ann. Hum. Genet.*, **66**: 183-193 (2002).

30) Bailey-Dell, K. J., Hassel, B., Doyle, L. A. and Ross, D. D.: Promoter characterization and genomic organization of the human breast cancer resistance protein (ATP-binding cassette transporter G2) gene. *Biochim. Biophys. Acta.*, **1520**: 234-241 (2001).

31) Zhou, Q., Sparreboom, A., Tan, E. H., Cheung, Y. B., Lee, A., Poon, D., Lee, E. J. and Chowbay, B.: Pharmacogenetic profiling across the irinotecan pathway in Asian patients with cancer. *Br. J. Clin. Pharmacol.*, **59**: 415-424 (2005).

32) Wang, N., Akey, J. M., Zhang, K., Chakraborty, R. and Jin, L.: Distribution of recombination crossovers and the origin of haplotype blocks: the interplay of population history, recombination, and mutation. *Am. J. Hum. Genet.*, **71**: 1227-1234 (2002).

33) Gabriel, S. B., Schaffner, S. F., Nguyen, H., Moore, J. M., Roy, J., Blumenstiel, B., Higgins, J., DeFelice, M., Lochner, A., Faggart, M., Liu-Cordero, S. N., Rotimi, C., Adeyemo, A., Cooper, R., Ward, R., Lander, E. S., Daly, M. J. and Altshuler, D.: The structure of haplotype blocks in the human genome. *Science*, **296**: 2225-2259 (2002).

34) Miwa, M., Tsukahara, S., Ishikawa, E., Asada, S., Imai, Y. and Sugimoto, Y.: Single amino acid substitutions in the transmembrane domains of breast cancer resistance protein (BCRP) alter cross resistance patterns in transfectants. *Int. J. Cancer*, **107**: 757-763 (2003).

35) Zhang, K., Calabrese, P., Nordborg, M. and Sun, F.: Haplotype block structure and its applications to association studies: power and study designs. *Am. J. Hum. Genet.*, **71**: 1386-1394 (2002).

BIOCHEMICAL PHARMACOLOGY 71 (2006) 1377–1385

available at www.sciencedirect.com

SCIENCE DIRECT

journal homepage: www.elsevier.com/locate/biochempharm

Oxidative metabolism of 5-methoxy-N, N-diisopropyltryptamine (Foxy) by human liver microsomes and recombinant cytochrome P450 enzymes

Shizuo Narimatsu [a,*], *Rei Yonemoto* [a], *Keita Saito* [a], *Kazuo Takaya* [b], *Takuya Kumamoto* [b], *Tsutomu Ishikawa* [b], *Masato Asanuma* [c], *Masahiko Funada* [d], *Kimio Kiryu* [e], *Shinsaku Naito* [e], *Yuzo Yoshida* [f], *Shigeo Yamamoto* [g], *Nobumitsu Hanioka* [a]

[a] *Laboratory of Health Chemistry, Graduate School of Medicine, Dentistry and Pharmaceutical Sciences, Okayama University, 1-1-1 Tsushima-naka, Okayama 700-8530, Japan*

[b] *Laboratory of Medicinal Organic Chemistry, Graduate School of Pharmaceutical Sciences, Chiba University, 1-33 Yayoi, Inage, Chiba 263-8522, Japan*

[c] *Department of Brain Science, Okayama University, Graduate School of Medicine, Dentistry and Pharmaceutical Sciences, 2-5-1 Shikata, Okayama 700-8558, Japan*

[d] *Division of Drug Dependence, National Institute of Mental Health, National Center of Neurology and Psychiatry, 4-1-1 Ogawa-Higashi, Kodaira 187-8502, Japan*

[e] *Division of Pharmacology, Drug Safety and Metabolism, Otsuka Pharmaceutical Factory Inc., Naruto, Tokushima 772-8601, Japan*

[f] *School of Pharmaceutical Sciences and Institute for Bioscience, Mukogawa Women's University, Nishinomiya, Hyogo 663-8179, Japan*

[g] *Laboratory of Biomolecular Sciences, Graduate School of Medicine, Dentistry and Pharmaceutical Sciences, Okayama University, 1-1-1 Tsushima-naka, Okayama 700-8530, Japan*

ARTICLE INFO

Article history:
Received 7 December 2005
Accepted 24 January 2006

Keywords:
Foxy
5-MeO-DIPT
5-OH-DIPT
5-MeO-IPT
CYP2D6
CYP1A2
CYP2C8
CYP3A4

ABSTRACT

In vitro quantitative studies of the oxidative metabolism of (5-methoxy-N,N-diisopropyltryptamine, 5-MeO-DIPT, Foxy) were performed using human liver microsomal fractions and recombinant CYP enzymes and synthetic 5-MeO-DIPT metabolites. 5-MeO-DIPT was mainly oxidized to O-demethylated (5-OH-DIPT) and N-deisopropylated (5-MeO-IPT) metabolites in pooled human liver microsomes. In kinetic studies, 5-MeO-DIPT O-demethylation showed monophasic kinetics, whereas its N-deisopropylation showed triphasic kinetics. Among six recombinant CYP enzymes (CYP1A2, CYP2C8, CYP2C9, CYP2C19, CYP2D6 and CYP3A4) expressed in yeast or insect cells, only CYP2D6 exhibited 5-MeO-DIPT O-demethylase activity, while CYP1A2, CYP2C8, CYP2C9, CYP2C19 and CYP3A4 showed 5-MeO-DIPT N-deisopropylase activities. The apparent K_m value of CYP2D6 was close to that for 5-MeO-DIPT O-demethylation, and the K_m values of other CYP enzymes were similar to those of the low-K_m (CYP2C19), intermediate-K_m (CYP1A2, CYP2C8 and CYP3A4) and high-K_m phases (CYP2C9), respectively, for N-deisopropylation in human liver microsomes. In inhibition studies, quinidine (1 μM), an inhibitor of CYP2D6, almost completely inhibited human liver microsomal 5-MeO-DIPT O-demethylation at a substrate concentration of 10 μM.

* *Corresponding author.* Tel.: +81 86 251 7942; fax: +81 86 251 7942.
E-mail address: shizuo@pharm.okayama-u.ac.jp (S. Narimatsu).
0006-2952/$ – see front matter
doi:10.1016/j.bcp.2006.01.015

Abbreviations:
CYP, cytochrome P450
OR, NADPH-cytochrome P450 reductase
5-MeO-DIPT, 5-methoxy-*N*,*N*-diisopropyltryptamine
5-MeO-IPT, 5-methoxy-*N*-ispropyltryptamine
5-OH-DIPT, 5-hydroxy-*N*,*N*-diisopropyltryptamine
G-6-P, glucose 6-phosphate
HPLC, high-performance liquid chromatography
LC/MS, liquid chromatography–mass spectrometry
PCR, polymerase chain reaction

Furafylline, a CYP1A2 inhibitor, quercetin, a CYP2C8 inhibitor, sulfaphenazole, a CYP2C9 inhibitor and ketoconazole, a CYP3A4 inihibitor (5 μM each) suppressed about 60%, 45%, 15% and 40%, respectively, of 5-MeO-DIPT *N*-deisopropylation at 50 μM substrate. In contrast, omeprazole (10 μM), a CYP2C19 inhibitor, suppressed only 10% of *N*-deisopropylation by human liver microsomes, whereas at the same concentration the inhibitor suppressed the reaction by recombinant CYP2C19 almost completely. These results indicate that CYP2D6 is the major 5-MeO-DIPT *O*-demethylase, and CYP1A2, CYP2C8 and CYP3A4 are the major 5-MeO-DIPT *N*-deisopropylase enzymes in the human liver.

1. Introduction

Various kinds natural and synthetic hallucinogenic indolethylamines have been produced and abused worldwide, including in Japan [1,2]. Among the many hallucinogenic indolethylamines, the following five compounds are legally controlled in Japan: *N*,*N*-dimethyltryptamine, *N*,*N*-diethyltryptamine, α-ethyltryptamine, psilocine and psilocybin [2]. In addition, α-methyltryptamine and 5-methoxy-*N*,*N*-diisopropyltryptamine (5-MeO-DIPT, Foxy) have newly come under legal control as of 2005.

5-MeO-DIPT is one of the designer drugs, and its properties such as pharmacological activities and toxicities have not been fully elucidated [3]. 5-MeO-DIPT is taken orally because it is resistant to the degradation by monoamine oxidase [3]. It is thought that 5-MeO-DIPT undergoes oxidative metabolism in the liver after oral intake. In fact, there are two case reports in which several oxidative metabolites were detected in human serum and urine samples [4,5] using gas chromatography–mass spectrometry (GC–MS) techniques. However, most of the oxidative metabolites of 5-MeO-DIPT were only speculated to be produced on the basis of fragment ions in the GC–MS analysis.

There have thus far been no quantitative reports describing detailed in vitro studies on the oxidative metabolism of 5-MeO-DIPT. In the present study, we therefore investigated the in vitro oxidative metabolism of 5-MeO-DIPT using human liver microsomal fractions and recombinant cytochrome P450 enzymes as enzyme sources, and synthetic metabolites of 5-MeO-DIPT as standards for analysis.

2. Materials and methods

2.1. Materials

5-MeO-DIPT was supplied by Dr. M. Funada, National Institute of Mental Health, National Center of Neurology and Psychiatry (Kodaira, Japan). Because this compound showed the purity of above 99% in ^{1}H NMR and HPLC, it was used without further purification. 5-Hydroxy-*N*,*N*-diisopropyltryptamine (5-OH-DIPT) and 5-methoxy-*N*-isopropyltryptamine (5-MeO-IPT) were synthesized as described below. Furafylline, quercetin, sulfaphenazole, omeprazole and quinidine were purchased from Sigma–Aldrich (St. Louis, MO); glucose 6-phosphate (G-6-P) and NADPH were from Oriental Yeast Co. (Tokyo, Japan). Ketoconazole was supplied by Dr. Y. Yoshida, School of Pharmaceutical Sciences, Mukogawa Women's University. Pooled human liver microsomal fractions were obtained from BD Biosciences Discovery Labware (Bedford, MA). Recombinant CYP2D6 [6] was expressed in yeast cells according to the published methods. Recombinant CYP1A2, CYP2C8, CYP2C9, CYP2C19 and CYP3A4 were expressed in yeast cells as described below. Insect cell microsomal fractions (Supersomes) expressing CYP3A4, cytochrome b_5 and NADPH-cytochrome P450 reductase (OR), and expressing CYP3A4 and OR (without cytochrome b_5) were purchased from Gentest (Woburn, MA).

2.2. Chemical synthesis of 5-OH-DIPT and 5-MeO-IPT

To a solution of 5-MeO-DIPT (50 mg, 0.18 mmol) in CH_2Cl_2 (2.0 ml), 1.0 M BBr_3 in CH_2Cl_2 (0.92 ml, 0.92 mmol) was added at −12 °C and the whole was stirred at −12 °C for 3 h. After cooling the reaction mixture with an ice bath, 30% aq. NaOH was added to pH 9–10 and the whole was extracted with a mixture of $CHCl_3$ and MeOH (9: 1, 1 × 10 ml, 3 × 5 ml). The combined organic layer was washed with brine (10 ml) and was dried over Na_2SO_4. The solvent was evaporated in vacuo and the residue was purified by column chromatography (NH silica, $CHCl_3$:MeOH:Et_3N = 20:1:0.1) to give pale yellow crystals (21 mg, 44%); m.p. 81–83 °C; IR (ATR, cm^{-1}) 3330; ^{1}H NMR (400 MHz, $CDCl_3$) δ (ppm): 1.12 (total 12H, d, J = 6.3 Hz, 4 × CH_3), 2.76, 2.84 (each 2H, m, 2 × CH_2), 3.17 (total 2H, m, 2 × CH), 6.77 (1H, dd, J = 8.8, 2.4 Hz, H-6), 7.01 (1H, d, J = 2.2 Hz, H-4), 7.03 (1H, d, J = 2.2 Hz, H-2), 7.21 (1H, d, J = 8.8 Hz, H-7), 7.83 (1H, s, NH, exchangeable with D_2O); ^{13}C NMR (125 MHz, $CDCl_3$) δ (ppm): 20.3, 27.5, 47.0, 49.7, 50.6, 103.2, 111.8, 112.0, 122.3, 128.2, 131.3, 150.1; HRFABMS found: 261.1982 (calculated for $C_{16}H_{25}N_2O$:261.1967). These analytical data supported the conclusion that the synthesized compound was 3-(2-diisopropylaminoethyl)-1H-indol-5-ol (5-hydroxy-*N*,*N*-diisopropyltryptamine, 5-OH-DIPT) (Fig. 1).

To a solution of 5-methoxytryptamine (93 mg, 0.49 mmol) in MeOH (1.0 ml), 36% HCl (0.13 ml, 1.31 mmol), acetone

(1.08 ml, 14.7 mmol), and $NaBH_3CN$ (90%, 117 mg, 1.68 mmol) were added at 0 °C and the mixture was stirred at room temperature for 73 h. Ten percent aqueous KOH (2.0 ml) was added to pH 8–9 and the whole was extracted with CH_2Cl_2 (1 × 5 ml, 1 × 3 ml, 2 × 2 ml). The combined organic layer was washed with brine and was dried over K_2CO_3. The solvent was evaporated in vacuo and the residue was purified by column chromatography (NH silica, benzene:AcOEt:MeOH = 20:2:0.75) to give a reddish brown oil (86 mg, 76%); IR (ATR, cm^{-1}) 3200; ^1H NMR (400 MHz, $CDCl_3$) δ (ppm): 1.05 (6H, d, J = 6.2 Hz, 2 × CH_3), 2.82 (1H, quint. J = 6.2 Hz, CH), 2.94 (4H, s, 2 × CH_2), 3.85 (3H, s, OCH_3), 6.85 (1H, dd, J = 8.8, 2.4 Hz, H-6), 6.98 (1H, d, J = 2.4 Hz, H-4), 7.06 (1H, d, J = 2.4 Hz, H-2), 7.13 (1H, d, J = 8.8 Hz, H-7), 8.51 (1H, s, NH, exchangeable with D_2O); ^{13}C NMR (125 MHz, $CDCl_3$) δ (ppm): 22.8, 25.9, 47.4, 48.5, 55.9, 100.7, 111.8, 112.0, 113.4, 122.8, 129.8, 131.6, 153.7; HREIMS found: 232.1555 (calculated for $C_{13}H_{18}N_2O$:232.1575). These analytical data supported the conclusion that the synthesized compound was isopropyl-[2-(5-methoxy-1H-indol-3-yl)ethyl]amine (5-methoy-*N*-isopropyltryptamine, 5-MeO-IPT) (Fig. 1).

2.3. *Construction of CYP expression plasmids*

CYP1A2 cDNA for subcloning in expression vector pGYR1 was prepared by polymerase chain reaction (PCR) from pcDNA3.1/CYP1A2 plasmid [7] as a template using the forward primer, 5′-AAGCTTAAAAAAATGGCATTGTCCCAGTCT-3′, and the reverse primer, 5′-AAGCTTTCAGTTGATGGAGAAGCGCA-3′. The *Hin*dIII sites (marked with the solid lines) were introduced to the 5′-end of the start codon and the 3′-end of the stop codon to facilitate subcloning into pGYR1. A Kozak sequence (marked in italics) was also introduced upstream of the start codon to achieve high expression of the protein in yeast cells. CYP2C8 and CYP2C9 cDNAs were amplified from human adult normal liver QuickClone cDNA (BD Biosciences Clontech, Mountain View, CA). The nucleotide sequences used for the forward and reverse primers were 5′-CCCAAGCTTAAAAAAATGGAACCTTTTGTGGTCCTGG-3′ and 5′-TTCAAGCTTCTCGAGTTCAGACAGGGATGAAGCA-GAT-3′ for CYP2C8, and 5′-AAGCTTAAAAAAATGGATTCTC-TTGTGGTC-3′ and 5′-AAGCTTTCAGACAGGAATGAAGCACA-3′ for CYP2C9. The PCR products were directly introduced into pGEM-T vector (Promega, Madison, WI) using the TA cloning system, resulting in pGEM-T/CYP1A2, pGEM-T/CYP2C8 and pGEM-T/CYP2C9. CYP2C19 cDNA cloned into pBluescript SK (±) (pBluescript/CYP2C19) was supplied by Dr. J. Goldstein (NIEHS, Research Triangle, NC). The cDNA containing the *Hin*dIII sites and Kozak sequence was amplified by PCR from pcDNA3.1/CYP2C19 as a template using the forward primer 5′-CCCAAGCT-TAAAAAAATGGATCCTTTTGTGGTCC-3′ and the reverse primer 5′-GGAAAGCTTAGGAGCAGCCAGACCATCTGT-3′. The PCR product was digested with *Hin*dIII and ligated into the same restriction enzyme site of pcDNA3.1 (+), resulting in pcDNA3.1/CYP2C19. pGEM-T/CYP1A2, pGEM-T/CYP2C8, pGEM-T/CYP2C9 and pcDNA3.1/CYP2C19 plasmids were sequenced in both the forward and reverse directions using ABI BigDye terminator cycle sequencing reaction kit v3.1 (Applied Biosystems, Piscaway, NJ) to confirm that there were no PCR errors. The DNA fragments corresponding to CYP1A2, CYP2C8, CYP2C9 and CYP2C19 were cut out with *Hin*dIII from the pGEM-T or pcDNA3.1 (+) plasmid and were subsequently subcloned into the pGYR1 yeast expression vector digested with *Hin*dIII. The expression plasmids were sequenced to verify the correct orientation with respect to the promoter for pGYR1. The construction of CYP2D6 expression plasmid (pGYR1/CYP2D6) was described previously [8]. CYP3A4 expression plasmid (pGYR1/CYP3A4) was supplied by Dr. Y. Saito (National Institute of Health Sciences, Tokyo, Japan).

2.4. *Expression of CYP enzymes*

The pGYR1 vectors containing CYP cDNAs were used to transform *Saccharomyces cerevisiae* AH22 by the lithium acetate

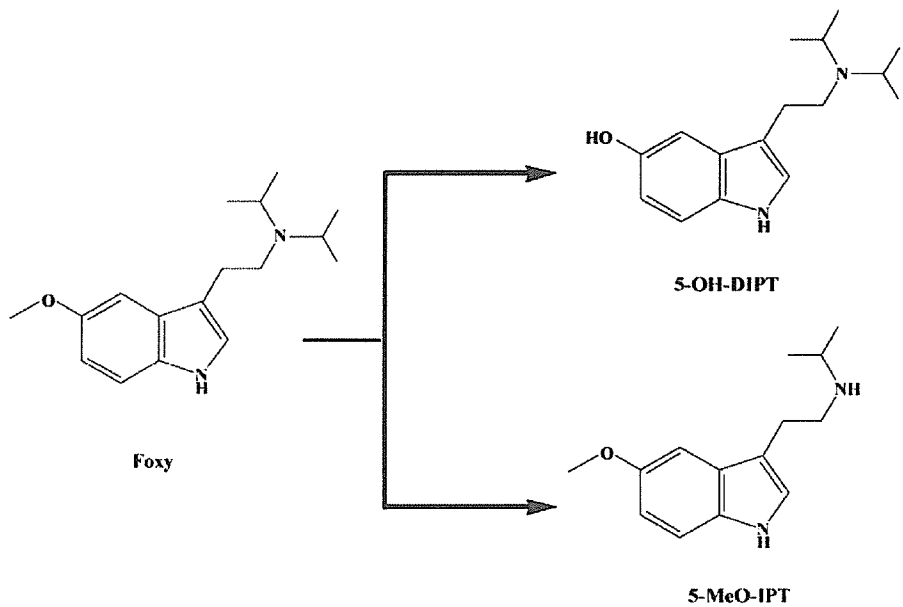

Fig. 1 – Major metabolic pathways of 5-MeO-DIPT.

method, and the cultivation of yeast transformants was performed as described [9]. Microsomes from yeast were prepared as described previously [10]. The yeast cell microsomal content of each recombinant CYP enzyme was as follows: CYP1A2 (13.5 pmol/mg protein), CYP2C8 (95.3 pmol/mg protein), CYP2C9 (76.0 pmol/mg protein), CYP2C19 (41.8 pmol/mg protein), CYP2D6 (65.0 pmol/mg protein) and CYP3A4 (49.1 pmol/mg protein).

2.5. Measurement of oxidation activities of 5-MeO-DIPT

A typical reaction mixture consisted of G-6-P (10 mM, final concentration), NADPH (1 mM), $MgCl_2$ (10 mM), EDTA (0.2 mM), microsomal fraction from human liver or yeast cells expressing CYP enzyme (0.08–0.12 mg protein) and the substrate (0.1–1000 μM) in 50 mM potassium phosphate buffer (pH 7.4) in a 1.5-ml Eppendorf-type tube (a final volume of 200 μl). Following preincubation at 37 °C for 5 min, the reaction was started by adding microsomal fractions from human livers or yeast cells expressing CYP enzymes, continued for 5–10 min, and stopped by adding aqueous 2 M phosphoric acid (10 μl) and 20 mM ascorbic acid (20 μl), vigorously mixing with a Vortex mixer, and chilling in an ice bath for 10 min. The tube was then centrifuged at 14,000 × *g* at 4 °C for 10 min, and the supernatant was passed through a 0.45-μm membrane filter (Millipore, Billerica, MA). An aliquot (20 μl) was subjected to high-performance liquid chromatography (HPLC) under the conditions described below. Calibration curves of 5-OH-DIPT and 5-MeO-IPT were made by spiking ice-cold reaction medium with known amounts of the synthetic compounds, followed by the addition of aqueous 2 M phosphoric acid and 20 mM ascorbic acid and treatment as described above. The detection limits for 5-OH-DIPT and 5-MeO-IPT were 0.5 and 1.0 pmol/ml, with a signal-to-noise ratio of 3 in both cases. The intra- and inter-day coefficients of variation did not exceed 10% for any assay.

2.6. HPLC conditions

The HPLC apparatus consisted of a Hitachi L-2130 pump, an L-2480 fluorescence detector, an L-2300 column oven, a D-2000 system manager (version 1.1) and a Rheodyne type 7725i injector. Other conditions were as follows: column, Inertsil C8 (150 mm × 4.6 mm i.d., GL Sciences, Co. Ltd., Tokyo, Japan); column temperature, 40 °C; detection, fluorescence excitation/emission wavelength, 280/340 nm. The mobile phase used was a linear gradient system consisting of (A) 20 mM ammonium acetate (pH 4.0)/acetonitrile (92:8 v/v) and (B) 20 mM ammonium acetate (pH 4.0)/acetonitrile (80:20) as follows: 0–3 min, (A) 100%; 3–15 min, from (A) 100% to (B) 100%; 15–25 min, (B) 100%; 25–30 min, from (B) 100% to (A) 100%; 30–40 min, (A) 100% at a flow rate of 0.9 ml/min.

2.7. LC/MS conditions

LC/MS analysis was performed using a JMS-700 MStation (JEOL, Tokyo, Japan). HPLC conditions were: column, Inertsil ODS-3 (150 mm × 2.1 mm i.d., GL Science); mobile phase, aqueous 0.1% TFA/acetonitrile (84:16 v/v); column temperature, 40°; flow rate, 0.2 ml/min; injection volume, 20 μl; detection, fluorescence excitation/emission wavelength, 280/340 nm. MS conditions were: ionization mode, ESI(+); needle voltage, 2.0 kV; ring voltage, 45 V; orifice voltage, 0 V; the temperatures of the orifice and desolvating plate were 80 and 220 °C; the resolution of the mass spectrometer was set at 1000 or 3000; collision gas, He.

2.8. Others

Total holo-CYP contents in yeast cell microsomal fractions were spectrophotometrically measured by assessing the reduced carbon monoxide spectra according to the method of Omura and Sato [11] using 91 mM^{-1} cm^{-1} as the absorption coefficient. Protein concentration was determined by the method of Lowry et al. [12]. Kinetic parameters (apparent K_m and V_{max} values) were estimated by analyzing Michaelis–Menten plots or Eadie–Hofstee plots using the computer program Prism ver. 4.0 software (GraphPad Software, San Diego, CA).

3. Results

First, we examined the in vitro oxidative metabolism of 5-MeO-DIPT using pooled human liver microsomes from Caucasians. When 50 μM 5-MeO-DIPT was used as the substrate, two major metabolite peaks [M – 1 (retention time of 10.3 min) and M – 3 (15.1 min)] were observed on the HPLC chromatogram (Fig. 2). Because the retention times and fragmentation profiles of M – 1 and M – 3 coincided with those of 5-OH-DIPT and 5-MeOH-IPT synthetic standards in LC/MS analysis, M – 1 and M – 3 were identified as 5-OH-DIPT and 5-MeOH-IPT, respectively (Fig. 3).

Furthermore, two metabolite peaks [M – 2 (retention time 12.0 min) and M – 4 (17.7 min) in HPLC] were analyzed by LC/MS. The fragment ions were as follows: M – 2; *m/z* 291 (M + 1, 100%), 181 (42%), 140 (85%), 124 (18%): M – 4; *m/z* 305 (M + 1, 64%), 278 (18%), 204 (55%), 144 (100%). From the molecular ion (*m/z* 291), M – 2 is thought to be a monohy-

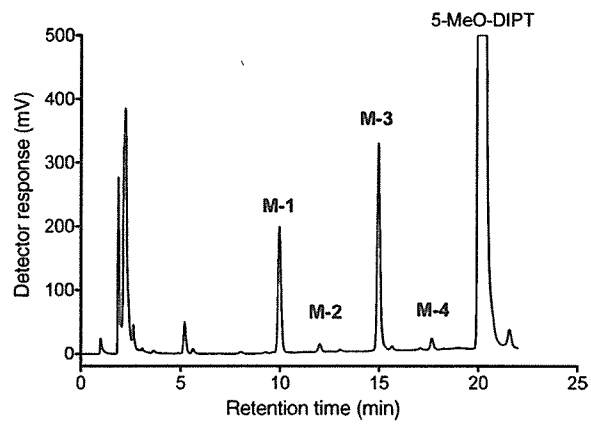

Fig. 2 – A typical HPLC chromatogram of 5-MeO-DIPT and its metabolites. The reaction mixture containing human liver microsomes and 5-MeO-DIPT (50 μM) was incubated in the presence of an NADPH-generating system and the metabolites formed were examined by HPLC under the conditions described in Section 2.

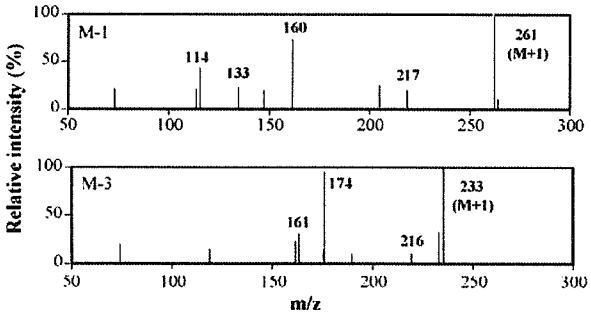

Fig. 3 – Mass fragment ions of M – 1 and M – 3. LC/MS conditions are given in Section 2.

droxylated 5-MeO-DIPT. It is feasible that M – 4 is a dehydrogenated product of dihydroxylated 5-MeO-DIPT.

It is reasonable to think that the formation of these metabolites was catalyzed by CYP enzymes in the liver microsomal fractions. We therefore examined what kinds of CYP enzymes were involved in the formation of M – 1 and M – 3 from 5-MeO-DIPT in human liver microsomes in the second step of this study. For this, we used six human recombinant CYP enzymes expressed in yeast cells: CYP1A2, CYP2C8, CYP2C9, CYP2C19, CYP2D6 and CYP3A4.

In this experiment, we employed two substrate concentrations (1 and 50 μM). All of the CYP enzymes except for CYP3A4 exhibited the capacity to oxidize 5-MeO-DIPT (Fig. 4). CYP3A4 expressed in yeast cells did not produce any metabolites in detectable amounts even at 50 μM substrate under the conditions used. We further examined the metabolic capacity of commercially available insect cell microsomal fractions (Supersomes) expressing CYP3A4, OR and cytochrome b_5. Interestingly, Supersomes co-expressing CYP3A4 with cytochrome b_5 exhibited considerable 5-MeO-DIPT N-deisopropylase but not O-demethylase activity, whereas Supersomes without cytochrome b_5 did not show any detectable activity (Fig. 4). As a result, among the six CYP enzymes tested, only CYP2D6 exhibited 5-MeO-DIPT O-demethylase activity, whereas all of the six recombinant enzymes showed 5-MeO-DIPT N-deisopropylase activitiy. The activities were ranked as CYP2C19 > CYP1A2 > CYP3A4 > CYP2C8 > CYP2C9 = CYP2D6.

Table 1 – Kinetic parameters for 5-MeO-DIPT oxidation by human liver microsomes

	K_m (μM)	V_{max} (pmol/min/mg protein)	V_{max}/K_m (μl/min/mg protein)
O-demethylation	5.0	140	27.9
N-deisopropylation			
Low-K_m phase	24	25	1.03
Intermediate-K_m phase	257	178	0.69
High-K_m phase	1201	409	0.34

Each value represents the mean of two determinations.

We then performed kinetic analysis using substrate concentrations ranging from 0.1 to 1000 μM and the pooled human microsomal fraction and the yeast cell microsomal fractions expressing recombinant CYP enzymes as enzyme sources. Only for CYP3A4, the Supersomes expressing CYP3A4, OR and cytochrome b_5 was employed. 5-MeO-DIPT O-demethylation by the pooled human liver microsomal fraction exhibited monophasic kinetics (Fig. 5A), whereas human liver microsomal N-deisopropylation showed triphasic kinetics (Fig. 5B). Table 1 summarizes the kinetic parameters. The apparent K_m value for monophasic 5-MeO-DIPT O-demethylation was calculated to be 5 μM, while the low-, intermediate- and high-K_m values for triphasic N-deisopropylation were calculated to be 24, 260 and 1200 μM, respectively.

For 5-MeO-DIPT O-demethylation, recombinant CYP2D6 yielded monophasic kinetics and an apparent K_m value of 2 μM. For 5-MeO-DIPT N-deisopropylation, CYP2C19, CYP3A4, CYP1A2, CYP2C8 and CYP2C9 showed monophasic kinetics, and gave K_m values of 35, 180, 260, 290 and 1660 μM, respectively (Table 2). These K_m values are similar to the values of the low-, intermediate- and high-K_m phases, respectively, of the human liver microsomal fraction (Table 1). In the case of N-

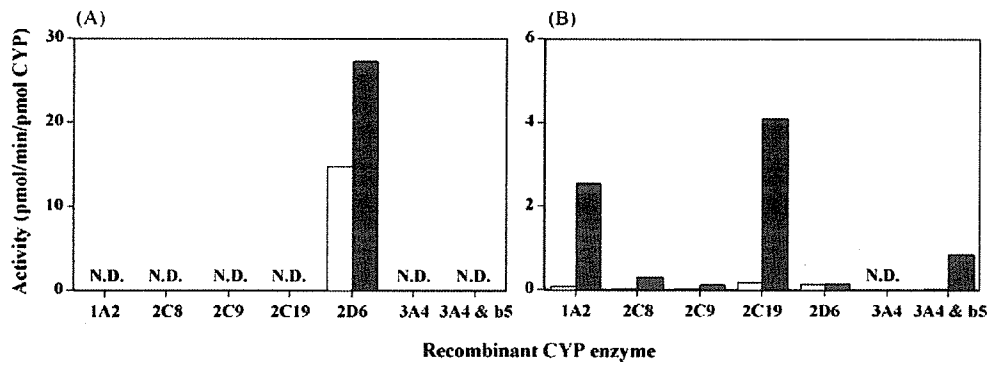

Fig. 4 – Comparison of 5-MeO-DIPT oxidation activities of recombinant CYP enzymes expressed in yeast or insect cells. For incubation, 5 pmol of each CYP enzyme was employed: (A) 5-MeO-DIPT O-demethylation; (B) 5-MeO-DIPT N-deisopropylation. Open columns, 5-MeO-DIPT 1 μM; closed columns, 5-MeO-DIPT 50 μM. Each value represents the mean of two determinations. 3A4 & b_5, Supersomes; N.D., not detectable.

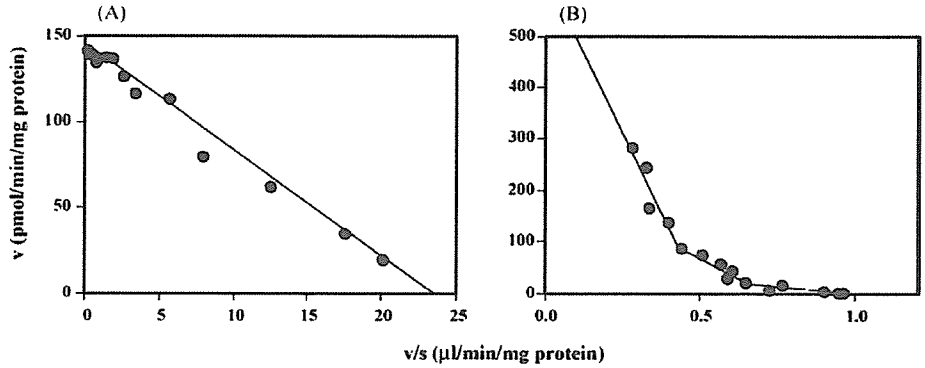

Fig. 5 – Kinetic analysis of 5-MeO-DIPT oxidation by human liver microsomes. (A) and (B) Eadie–Hofstee plots for 5-MeO-DIPT *O*-demethylation and *N*-deisopropylation, respectively.

deisopropylation by CYP2D6, precise kinetic parameters were not calculated because of the low activities.

In the third step of the present study, we examined the effects of inhibitors of the CYP enzymes on the oxidative metabolism of 5-MeO-DIPT in human liver microsomes to estimate the contribution of the CYP enzymes. For this, we employed furafylline [13], quercetin [14], sulfaphenazole [15], omeprazole [16], quinidine [17] and ketoconazole [18] as specific inhibitors of CYP1A2, CYP2C8, CYP2C9, CYP2C19, CYP2D6 and CYP3A4, respectively. For 5-MeO-DIPT *O*-demethylation by human liver microsomes, quinidine showed a concentration-dependent inhibition. Over 95% of the activity was suppressed by the inhibitor even at 5 μM (Fig. 6A).

Furafylline and quercetin inhibited human liver microsomal 5-MeO-DIPT *N*-deisopropylation in a concentration-dependent manner, but about 30–40% of the activity remained even at the highest concentration of the inhibitors (Fig. 6B and C). Sulfaphenazole also caused a concentration-dependent

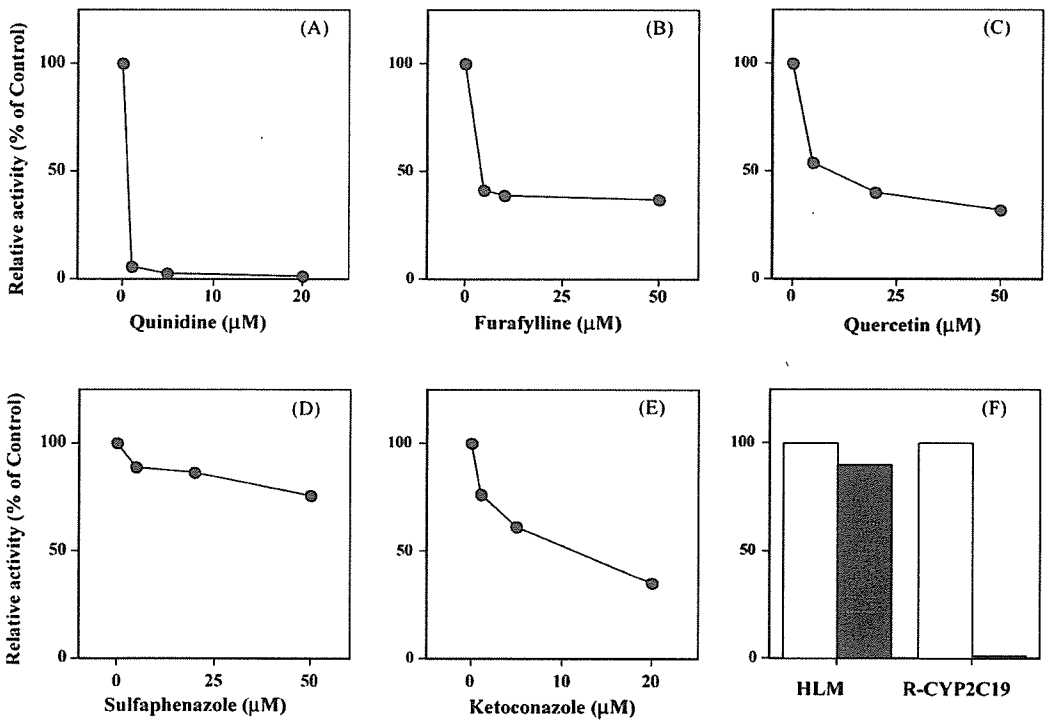

Fig. 6 – Effects of various CYP inhibitors on 5-MeO-DIPT oxidation by human liver microsomes: (A) quinidine (0, 0.5, 5 and 20 μM) as CYP2D6 inhibitor; (B) furafylline (0, 5, 10 and 50 μM) as CYP1A2 inhibitor; (C) quercetin (0, 5, 20 and 50 μM); (D) sulfaphenazole (0, 5, 20 and 50 μM) as CYP2C9 inhibitor; (E) ketoconazole (0, 1, 5 and 20 μM) as CYP3A4 inhibitor; (F) omeprazole (10 μM) as CYP2C19 inhibitor. (A) 5-MeO-DIPT *O*-demethylation; (B), (C), (D), (E) and (F) 5-MeO-DIPT *N*-deisopropylation. The substrate concentrations used were 10 μM for (A) and 50 μM for (B), (C), (D), (E) and (F). Each value represents the mean of two determinations. HLM, human liver microsomes.

Table 2 – Kinetic parameters for 5-MeO-DIPT oxidation by recombinant CYP enzymes expressed in yeast cells

	K_m (μM)	V_{max} (pmol/min/pmol CYP)	V_{max}/K_m (μl/min/pmol CYP)
O-demethylation			
CYP2D6	2.0	29.8	14.8
N-deisopropylation			
CYP1A2	263	9.4	0.04
CYP2C8	291	1.7	0.006
CYP2C9	1663	4.2	0.003
CYP2C19	35	6.9	0.19
CYP3A4[a]	184	4.4	0.02

Each value represents the mean of two determinations.
[a] Data from Supersomes in which CYP3A4 and cytochrome b_5 were co-expressed.

inhibition, but suppressed only 25% of human liver microsomal 5-MeO-DIPT N-deisopropylation at the highest concentration of 50 μM (Fig. 6D). Ketoconazole suppressed 40% and 65% of the N-deisopropylase activity at final concentrations of 5 and 20 μM, respectively (Fig. 6E). Omeprazole (10 μM) suppressed only 10% of 5-MeO-DIPT N-deisopropylation by pooled human liver microsomes, though this inhibitor at the same concentration suppressed the 5-MeO-DIPT N-deisopropylation by recombinant CYP2C19 almost completely (Fig. 6F).

4. Discussion

There have hitherto been no reports of the quantitative assays using authentic samples of 5-MeO-DIPT metabolites to study the formation of 5-MeO-DIPT metabolites. We therefore chemically synthesized the two compounds, 5-OH-DIPT and 5-MeO-IPT, and conducted a quantitative analysis of the formation of these metabolites. Using these synthetic samples, we examined the in vitro oxidative metabolism of 5-MeO-DIPT by human liver microsomes and recombinant CYP enzymes. As expected, 5-MeO-DIPT was biotransformed into 5-OH-DIPT and 5-MeO-IPT as major metabolites by human liver microsomes under the conditions used. Two other metabolites were also tentatively identified as monohydroxylated 5-MeO-DIPT and a dehydrogenated product of dihydroxylated 5-MeO-DIPT on the basis of the data from LC/MS analysis.

In a preliminary HPLC experiment, we compared the amounts of 5-OH-DIPT and 5-MeO-IPT formed with the amount of 5-MeO-DIPT consumed during the incubation of the substrate (10 μM) under similar conditions to those employed here. The results indicated that at least 95% of substrate consumption was explained by the formation of the two major metabolites (data not shown). Therefore, it is reasonable to think that 5-OH-DIPT and 5-MeO-IPT are the major metabolites in human liver microsomes at around 10 μM substrate concentrations (Fig. 1).

Human liver microsomal 5-MeO-DIPT O-demethylation and N-deisopropylation exhibited monophasic and triphasic kinetics, respectively. We have been studying the relationships between protein structures and enzymatic functions of major drug-metabolizing CYP enzymes such as CYP1A2 [19] and CYP2D6 [20,21]. Using the yeast cell expression systems of CYP1A2, CYP2C8, CYP2C9, CYP2C19, CYP2D6 and CYP3A4 constructed so far in this laboratory, we examined the metabolic capacities of these recombinant enzymes for the oxidation of 5-MeO-DIPT.

Among the recombinant enzymes, only CYP2D6 showed considerable 5-MeO-DIPT O-demethylase activity. This reaction in human liver microsomes yielded monophasic kinetics, and was almost completely suppressed by quinidine as a specific inhibitor of CYP2D6. The apparent K_m value (2 μM) for the recombinant CYP2D6 was similar to that (5 μM) for the human liver microsomes. These results indicate that 5-MeO-DIPT O-demethylation was mainly mediated by CYP2D6 in human livers.

In contrast, the two CYP enzymes (CYP1A2 and CYP2C19) in the yeast cell expression system exhibited considerable 5-MeO-DIPT N-deisopropylase activities. The activities of CYP2C8, CYP2C9 and CYP2D6 were much lower than those of CYP1A2 and CYP2C19. Interestingly, yeast cell microsomal CYP3A4 did not show any detectable activity for either O-demethylation or N-deispropylation. Before coming to a conclusion, we further examined the metabolic capacity of Supersomes expressing CYP3A4, OR and cytochrome b_5, because it is well known that co-existence of cytochrome b_5 increases the oxidation capacity of CYP3A4 for its substrates [22,23]. As expected, Supersomes co-expressing CYP3A4 with cytochrome b_5 exhibited considerable 5-MeO-DIPT N-demethylase activity, whereas Supersomes without cytochrome b_5 did not.

The apparent K_m values for CYP2C19 (35 μM), CYP3A4 (180 μM), CYP1A2 (260 μM), CYP2C8 (290 μM) and CYP2C9 (1700 μM) seem to correspond to those for human liver microsomal low- (24 μM), intermediate- (260 μM) and high-K_m (1200 μM) phases, respectively. To confirm the involvement of these CYP enzymes in human liver microsomal 5-MeO-DIPT N-deisopropylation, the effects of furafylline, quercetin, sulfaphenazole, omeprazole and ketoconazole were examined as specific inhibitors for CYP1A2, CYP2C8, CYP2C9, CYP2C19 and CYP3A4, respectively. Among them, furafylline, quercetin and ketoconazole exerted considerable inhibitory effects at relatively low concentrations (several μM).

We employed quercetin as the inhibitor of CYP2C8 in the present study, however, this compound was reported to inhibit the metabolic activities of CYP1A2, CYP2C19 and CYP3A4 as well [24]. Therefore, quercetin could suppress the activities not only of CYP2C8 but also of CYP1A2 and CYP3A4 in 5-MeO-DIPT N-deisopropylation by human liver microsomal fraction in this study. Inhibitory effect of sulfaphenazole was found to be weak as compared to those of furafylline and ketoconazole. Interestingly, the inhibitory effect of omeprazole was very weak under the conditions used. In this case, we employed an inhibitor concentration of 10 μM, which was sufficient to suppress the bufuralol 1″-hydroxylase activities of CYP2C19 in our previous studies [25]. In fact, 10 μM omeprazole completely suppressed 5-MeO-DIPT N-deisopropylation by recombinant CYP2C19 in the present study.

Other drug-metabolizing-type CYP enzymes such as CYP2E1, CYP2A6 and CYP2B6 could also be involved in the oxidation of 5-MeO-DIPT in the human liver. In another

preliminary experiment, we found that diethyldithiocarbamate (5, 20 and 100 μM final concentrations) as CYP2E1 inhibitor [26] did not affect 5-MeO-DIPT oxidation by the pooled human liver microsomal fraction (data not shown). Ono et al. [27] reported that diethyldithiocarbamate inhibits the metabolic activities of CYP2A6 and CYP2C19 in addition to that of CYP2E1. Furthermore, furafylline and ketoconazole (5 μM each) suppressed 60% and 40%, respectively, of human liver microsomal 5-MeO-DIPT *N*-deisopropylation under the conditions employed. CYP3A4 is the most abundant CYP enzyme followed by CYP2C and CYP1A2 in the human liver [28]. These results indicate that CYP1A2, CYP2C8 and CYP3A4 are the major 5-MeO-DIPT *N*-deisopropylases in the human liver at substrate concentrations around 50 μM or less.

The present results of the measurement of enzyme activities and the effects of inhibitors indicated that human liver microsomal 5-MeO-DIPT *O*-demethylation is mainly mediated by CYP2D6, whereas *N*-deisopropylation is mediated mainly by CYP1A2 and CYP3A4, and also by CYP2C8, CYP2C9 and CYP2C19, at least in part. The major contribution of CYP2D6 to 5-MeO-DIPT *O*-demethylation is predictable from the previous findings of Yu et al. [29,30] on the role of CYP2D6 in 5-MeO-tryptamine metabolism. It should be noted that though CYP2C19 exhibited the highest activity as 5-MeO-DIPT *N*-deisopropylase among the six recombinant CYP enzymes examined, its contribution was thought to be relatively low in the reaction by the pooled human liver microsomal fractions used in the present study.

The kinetic parameters, particularly the clearance (V_{max}/K_m) values, indicate that as compared to *N*-deisopropylation, *O*-demethylation might contribute to a much greater extent to the oxidative metabolism of 5-MeO-DIPT. The present results together with previous in vivo and in vitro findings cast considerable light on the metabolic fate of 5-MeO-DIPT in the human body. However, the toxicity of 5-MeO-DIPT and related compounds, including the metabolites of 5-MeO-DIPT, remain to be elucidated. If only the parent compound, 5-MeO-DIPT, has psychotomimetic activity and 5-MeO-DIPT *O*-demethylation is mediated mainly by CYP2D6, poor metabolizers who are deficient for functional CYP2D6 may show higher sensitivity to, or toxicity of, 5-MeO-DIPT than extensive metabolizers having normal CYP2D6 functions. Further systematic studies will be needed to understand the relationship between the metabolism and toxicity of 5-MeO-DIPT.

In summary, in vitro quantitative studies on the oxidative metabolism of 5-MeO-DIPT were performed using human liver microsomal fractions, recombinant CYP enzymes and synthetic 5-MeO-DIPT metabolites. 5-MeO-DIPT was mainly oxidized to *O*-demethylated (5-OH-DIPT) and *N*-deisopropylated (5-MeO-IPT) metabolites in pooled human liver microsomes. Kinetic analysis revealed that 5-MeO-DIPT *O*-demethylation showed monophasic kinetics, whereas *N*-deisopropylation gave triphasic kinetics. Among the six recombinant CYP enzymes examined, only CYP2D6 exhibited 5-MeO-DIPT *O*-demethylase activity, and CYP1A2, CYP2C8, CYP2C9, CYP2C19 and CYP3A4 showed 5-MeO-DIPT *N*-deisopropylase activities. The apparent K_m value of CYP2D6 was close to that for 5-MeO-DIPT *O*-demethylation, and the K_m value of other CYP enzymes were similar to those of the low-K_m (CYP2C19), intermediate-K_m (CYP1A2, CYP2C8 and CYP3A4) and high-K_m (CYP2C9) phases, respectively, for *N*-deisopropylation in human liver microsomes. These results together with the results of the inhibitory studies indicate that CYP2D6 is the major 5-MeO-DIPT *O*-demethylase and CYP1A2, CYP2C8 and CYP3A4 are the major *N*-deisopropylase enzymes in the human liver.

Acknowledgments

We would like to express our gratitude to Dr. Joyce A. Goldstein, National Institutes of Environmental Health Sciences, Research Triangle Park, NC, for her kind gift of CYP2C19 cDNA. This study was supported in part by a grant from the Japan Research Foundation for Clinical Pharmacology.

REFERENCES

[1] Ishida T, Kudo K, Kiyosghima A, Inoue H, Tsuji A, Ikeda N. Sensitive determination of alfa-methyltryptamine (AMT) and 5-methoxy-*N*,*N*-diisopropyltryptamine (5MeO-DIPT) in whole blood and urine using gas chromatography–mass spectrometry. J Chromatogr B 2005;823:47–52.
[2] Kikura-hanajiri R, Hayashi M, Saisho K, Goda Y. Simultaneous determination of nineteen hallucinogenic tryptamines/β-calbolines and phenethylamines usig gas chromatography–mass spectrometry and liquid chromatography–electrospray ionization-mass spectrometry. J Chromatogr B 2005;825:29–37.
[3] Shulgin AT, Carter MF. *N*,*N*-diisopropyltryptamine (DIPT) and 5-methoxy-*N*,*N*-diisopropyltryptamine (5-MeO-DIPT), two orally active tryptamine analogs with CNS activity. Commun Psychopharmacol 1980;4:363–9.
[4] Meatherall R, Sharma P. Foxy, a designer tryptamine hallucinogen. J Anal Toxicol 2003;27:313–7.
[5] Wilson JM, McGeorge F, Smalinske S, Meatherall R. A foxy intoxication. Forensic Sci Int 2005;148:31–6.
[6] Tsuzuki D, Takemi C, Yamamoto S, Tamagake K, Imaoka S, Funae Y, et al. Functional evaluation of cytochrome P450 2D6 with Gly42Arg substitution expressed in *Saccharomyces cerevisiae*. Pharmacogenetics 2001;11: 709–18.
[7] Saito Y, Hanioka N, Maekawa K, Isobe T, Tsuneto Y, Nakamura R, et al. Functional analysis of three CYP1A2 variants found in a Japanese population. Drug Metab Dispos 2006;33:1905–10.
[8] Sakaki T, Akiyoshi-Shibata M, Yabusaki Y, Ohkawa H. Organella-targeted expression of rat liver cytochrome P450c27 in yeast: genetically engineered alteration of mitochondrial P450 into a microsomal form creates a novel functional electron transport chain. J Biol Chem 1992;267:16497–502.
[9] Wan J, Imaoka S, Chow T, Hiroi T, Yabusaki Y, Funae Y. Expression of four rat CYP2D isoforms in *Saccharomyces cerevisiae* and their catalytic specificity. Arch Biochem Biophys 1997;348:383–90.
[10] Hichiya H, Takemi C, Tsuzuki D, Yamamoto S, Asaoka A, Suzuki S, et al. Complementary DNA cloning and characterization of cytochrome P450 2D29 from Japanese monkey liver. Biochem Pharmacol 2002;64:1101–10.
[11] Omura T, Sato R. The carbon monoxide-binding pigment of liver microsomes. I. Evidence for its hemoprotein nature. J Biol Chem 1964;239:2370–8.

[12] Lowry OH, Rosebrough NJ, Farr AL, Randall RJ. Protein measurement with the Folin phenol reagent. J Biol Chem 1951;193:265–75.
[13] Sesardic D, Boobis AR, Murray BP, Murray S, Segura J, Torre R, et al. Furafylline is a potent and selective inhibitor of cytochrome P450IA2 in man. Br J Clin Pharmacol 1990; 29:651–63.
[14] Rahman A, Korzekwa KR, Grogan J, Gonzalez FJ, Harris JW. Selective biotransformation of taxol to 6α-hydroxytaxol by human cytochrome P450 2C8. Cancer Res 1994;54:5543–6.
[15] Mancy A, Dijols S, Poli S, Guengerich P, Mansuy D. Interaction of sulfaphenazole derivatives with human liver cytochromes P450 2C: molecular origin of the specific inhibitory effects of sulfaphenazole on CYP 2C9 and consequences for the substrate binding site topology of CYP 2C9. Biochemistry 1996;35:16205–12.
[16] Ko JW, Sukhova N, Thacker D, Chen P, Flockhart DA. Evaluation of omeprazole and lansoprazole as inhibitors of cytochrome P450 isoforms. Drug Metab Dispos 1997;25: 853–62.
[17] Newton DJ, Wang RW, Lu AY. Cytochrome P450 inhibitors. Evaluation of specificities in the in vitro metabolism of therapeutic agents by human liver microsomes. Drug Metab Dispos 1995;23:154–8.
[18] Schmider J, Greenblatt DJ, von Moltke LL, Harmatz JS, Shader RI. N-demethylation of amitriptyline in vitro: role of cytochrome P-450 3A (CYP3A) isoforms and effect of metabolic inhibitors. J Pharmacol Exp Ther 1995;275:592–7.
[19] Narimatsu S, Oda M, Hichiya H, Isobe T, Asaoka K, Hanioka N, et al. Molecular cloning and functional analysis of cytochrome P450 1A2 from Japanese monkey liver: Comparison with marmoset cytochrome P450 1A2. Chem Biol Interact 2005;152:1–12.
[20] Masuda K, Hashimoto H, Tamagake K, Okuda Y, Tsuzuki D, Isobe T, et al. Changes in the enzymatic properties of CYP2D6 by the substitution of phenylalanine at position 120 by alanine. J Health Sci 2004;50:503–10.
[21] Masuda K, Tamagake K, Okuda Y, Torigoe F, Tsuzuki D, Isobe T, et al. Change in enantioselectivity in bufuralol 1″-hydroxylation by the substitution of phenylalanine-120 by alanine in cytochrome P450 2D6. Chirality 2005;17:34–7.
[22] Yamazaki H, Johnson WW, Ueng YF, Shimada T, Guengerich FP. Lack of electron transfer from cytochrome b_5 in stimulation of catalytic activities of cytochrome P450 3A4. Characterization of a reconstituted cytochrome P450 3A4/NADPH-cytochrome P450 reductase system and studies with apo-cytochrome b_5. J Biol Chem 1996;271:27438–44.
[23] Jushchyshyn MI, Hutzler JM, Schrag ML, Wienkers LC. Catalytic turnover of pyrene by CYP3A4: evidence that cytochrome b_5 directly induces positive cooperativity. Arch Biochem Biophys 2005;438:21–8.
[24] Zou L, Harkey MR, Henderson GL. Effects of herbal components on cDNA-expressed cytochrome P450 enzyme catalytic activity. Life Sci 2002;71:1579–89.
[25] Narimatsu S, Takemi C, Tsuzuki D, Kataoka H, Yamamoto S, Shimada S, et al. Stereoselective metabolism of bufuralol racemate and enantiomers in human liver microsomes. J Pharmacol Exp Ther 2002;303:172–8.
[26] Yamazaki H, Oda Y, Funae Y, Imaoka S, Inui Y, Guengerich FP, et al. Participation of rat liver cytochrome P450 2E1 in the activation of N-nitrosodimethylamine and N-nitrosodiethylamine to products genotoxic in an acetyltransferase-overexpressing *Salmonella typhimurium* strain. Carcinogenesis 1992;13: 979–85.
[27] Ono S, Hatanaka T, Hotta H, Satoh T, Gonzalez FJ, Tsutsui M. Specificity of substrate and inhibitor probes for cytochrome P450s: evaluation of in vitro metabolism using cDNA-expressed human P450s and human liver microsomes. Xenobiotica 1996;26:681–93.
[28] Shimada T, Yamazaki H, Mimura M, Inui Y, Guengerich FP. Interindividual variations in human liver cytochrome P-450 enzymes involved in the oxidation of drugs, carcinogens and toxic chemicals: studies with liver microsomes of 30 Japanese and 30 Caucasians. J Pharmacol Exp Ther 1994;270:414–23.
[29] Yu AM, Idle JR, Byrd LG, Krausz KWA, Kupfer A, Gonzalez FJ. Regeneration of serotonin from 5-methoxytryptamine by polymorphic human CYP2D6. Pharmacogenetics 2003;13:173–81.
[30] Yu AM, Idle JR, Herraiz T, Kupfer A, Gonzalez FJ. Screening for endogenous substrates reveals that CYP2D6 is a 5-methoxyindolethylamine O-demethylase. Pharmacogenetics 2003;13:307–9.

BIOCHEMICAL PHARMACOLOGY 72 (2006) 1738–1748

available at www.sciencedirect.com

ScienceDirect

journal homepage: www.elsevier.com/locate/biochempharm

Cloning of a cDNA encoding a novel marmoset CYP2C enzyme, expression in yeast cells and characterization of its enzymatic functions

Shizuo Narimatsu [a,*], *Fumihiro Torigoe* [a], *Yumi Tsuneto* [a], *Keita Saito* [a], *Nobumitsu Hanioka* [a], *Kazufumi Masuda* [b], *Takashi Katsu* [b], *Shigeo Yamamoto* [c], *Shigeru Yamano* [d], *Takahiko Baba* [e], *Atsuro Miyata* [f]

[a] *Laboratory of Health Chemistry, Graduate School of Medicine, Dentistry and Pharmaceutical Sciences, Okayama University, 1-1-1 Tsushima-naka, Okayama 700-8530, Japan*

[b] *Laboratory of Pharmaceutical Physical Chemistry, Graduate School of Medicine, Dentistry and Pharmaceutical Sciences, Okayama University, 1-1-1 Tsushima-naka, Okayama 700-8530, Japan*

[c] *Department of Pharmaceutical Health Chemistry, Faculty of Pharmaceutical Sciences, Matsuyama University, 4-2 Bunkyo-cho, Matsuyama 790-8578, Japan*

[d] *Department of Hygienic Chemistry, Faculty of Pharmaceutical Sciences, Fukuoka University, 8-19-1 Nanakuma, Minami-ku, Fukuoka 814-0180, Japan*

[e] *Developmental Research Laboratories, Shionogi & Co., Ltd., 3-1-1 Futaba-cho, Toyonaka 561-0825, Japan*

[f] *Department of Pharmacology, Graduate School of Medical and Dental Sciences, Kagoshima University, 8-35-1 Sakuragaoka, Kagoshima 890-8544, Japan*

ARTICLE INFO

Article history:
Received 2 June 2006
Accepted 25 August 2006

Keywords:
Marmoset
CYP2C8
Yeast cell
Tolbutamide
Quercetin

Abbreviations:
CYP, cytochrome P450
TB, tolbutamide
PT, paclitaxel
DF, diclofenac
S-MP, S-mephenytoin
G-6-P, glucose 6-phosphate

ABSTRACT

We cloned a cDNA encoding a novel CYP2C enzyme, called P450 M-2C, from a marmoset liver. The deduced amino acid sequence showed high identities to those of human CYP2C8 (87%), CYP2C9 (78%) and CYP2C19 (77%). The P450 M-2C enzyme expressed in yeast cells catalyzed *p*-methylhydroxylation of only tolbutamide among four substrates tested, paclitaxel as a CYP2C8 substrate, diclofenac and tolbutamide as CYP2C9 substrates and S-mephenytoin as a CYP2C19 substrate. *p*-Methylhydroxylation of tolbutamide by marmoset liver microsomes showed monophasic kinetics, and the apparent K_m value (1.2 mM) for the substrate was similar to that of the recombinant P450 M-2C (1.8 mM). Although all of the recombinant human CYP2C8, CYP2C9 and CYP2C19 expressed in yeast cells catalyzed tolbutamide *p*-methylhydroxylation, the kinetic profile of CYP2C8 was most similar to that of P450 M-2C. Tolbutamide oxidation by the marmoset liver microsomes and the recombinant P450 M-2C was inhibited most effectively by quercetin, a CYP2C8 inhibitor, followed by omeprazole, a CYP2C19 inhibitor, whereas sulfaphenazole, a CYP2C9 inhibitor, was less potent under the conditions used. These results indicate that P450 M-2C is the major tolbutamide *p*-methylhydroxylase in the marmoset liver.

* *Corresponding author.* Tel.: +81 86 251 7942; fax: +81 86 251 7942.
E-mail address: shizuo@pharm.okayama-u.ac.jp (S. Narimatsu).

0006-2952/$ – see front matter © 2006 Elsevier Inc. All rights reserved.
doi:10.1016/j.bcp.2006.08.025

1. Introduction

Several kinds of monkeys such as rhesus monkeys, crab-eating monkeys, Japanese monkeys and marmoset monkeys, have been employed as one of experimental animals in research on drug metabolism and toxicity. The old-world monkeys, including rhesus monkeys, crab-eating monkeys and Japanese monkeys ranging through Africa, Europe and Asia, have disadvantages such as body sizes too big for easy handling and poor fertility. In contrast, marmoset monkeys, belonging to the new-world monkeys ranging through Central and South America are thought to be promising candidates for experimental animals, because of their small size, easy handling and breeding.

Cytochrome P450 (CYP) is a key enzyme for oxidative drug metabolism in mammals including humans and monkeys. CYP constitutes a superfamily and four CYP subfamilies, namely, CYP1, –2, –3 and –4, are mainly responsible for drug metabolism in humans [1–3]. Although CYP enzymes have been extensively characterized in humans and the old-world monkeys, relatively little information is available about the properties of CYP enzymes in marmoset monkeys.

Previous studies provided experimental evidence supporting the notion that pretreatment with chemical compounds such as phenobarbital [4], 3-methylcholanthrene, polychlorinated biphenyl [5], 2,3,7,8-tetrachlorodibenzo-*p*-dioxin [6,7] or isoniazide [8] induced CYP isoenzymes in marmosets. Using targeted anti-peptide antibodies, Schulz et al. [9] suggested the possible expression of CYP1A1, CYP1A2, CYP2A, CYP2B, CYP2C, CYP2E1 and CYP3A21 enzymes in marmosets. Moreover, the research group of Kamataki isolated cDNA clones encoding CYP1A2 [5], CYP2D19 and CYP3A21 [10] from marmoset livers, and characterized the enzymatic properties of CYP1A2 expressed in high-red yeast cells [5]. Recently, we also cloned cDNAs encoding CYP1A2 [11], CYP2D19 and CYP2D30 [12] from fresh marmoset livers, and expressed the proteins in yeast cells to examine their enzymatic functions. However, for prompt utilization of marmoset monkeys as experimental animals in the study of drug metabolism and toxicity, functional characterization of other drug-metabolzing enzymes in this species would be required. In the present study, we have cloned a cDNA encoding a novel CYP2C enzyme from marmoset liver, expressed the protein in yeast cells, and characterized its enzymatic functions.

2. Materials and methods

2.1. Materials

Peclitaxel (PT), tolbutamide (TB), quercetin, sulfaphenazole and omeprazole were purchased from Sigma Chemical Co. (St. Louis, MO); 6α-hydroxypaclitaxel was from Calbiochem (San Diego, CA), docetaxel trihydrate was from Toronto Research Chemicals Inc. (North York, Ontario, Canada); diclofenac (DF), *N*-phenylanthranilic acid, glucose 6-phosphate (G-6-P) dehydrogenase (from yeast) and NADPH were from Wako Pure Chemicals Co. (Osaka, Japan); 4′-hydroxydiclofenac, S-mephenytoin (S-MP) and 4′-hydroxymephenytoin were from Daiichi Chemical Co. (Tokyo, Japan); phenobarbital and chlorpropamide were from Tokyo Kasei Kogyo Co. (Tokyo, Japan). *p*-Methylhydroxytolbutamide was supplied from Dr. Takahiko Baba. Pooled human liver microsomes from donors (12 Caucasians and 1 Hispanic, 13 males, 4–62 years old; 9 females, 40–74 years old) were purchased from BD Biosciences Discovery Labware (Bedford, MA). Other chemical reagents or solvents used were of the highest quality commercially available.

2.2. Cloning of cDNA encoding a marmoset CYP2C enzyme

Total RNA was extracted from an adult female marmoset liver (2 years old, supplied from Kagoshima University) using an RNeasy mini kit (Qiagen, Hilden, Germany), and first-strand DNA was synthesized using an RNA PCR kit (Version 3.0, Takara Bio, Ohtsu, Japan) according to the manufacturer's instructions. A full length cDNA encoding a marmoset CYP enzyme was amplified by polymerase chain reaction (PCR) using the forward primer 5′-GTAAGAAGAGAAGTCTTCAATG-3′ and the reverse primer 5′-ATACAAGTGTTACCGAGTATGA-3′. These primers were designed based on the nucleotide sequence in the flanking regions of the crab-eating monkey CYP2C20 cDNA (GenBank accession no. S53046). The reaction mixtures (50 μl) contained 0.2 mM dNTPs, 1 mM $MgSO_4$, 1 U of KOD-plus DNA polymerase (Toyobo, Osaka, Japan) and each oligonucleotide primer at 0.5 μM. PCR consisted of 35 cycles of denaturation at 94 °C for 30 s, annealing at 50 °C for 30 s and extension at 68 °C for 100 s. The initial denaturation was performed at 94 °C for 120 s. The amplified product (1.5 kbp) was purified with a MinElute gel extraction kit (Qiagen), and the 5′- and 3′-ends of the coding region were sequenced in both the forward and reverse directions using ABI BigDye terminator cycle sequencing reaction kit v3.1 (Applied Biosystems, Piscaway, NJ).

The full-length cDNA thus obtained was modified by PCR amplification with 5′-AAGCTTAAAAAAATGGATCCTTTTGT-GGTCC-3′ and 5′-AAGCTTTCAGACAGGAATGAAGCAGATC-TG-3′ as primers under the conditions described above. *Hin*dIII sites (marked with solid lines) were introduced to the 5′-end of the start codon and the 3′-end of the stop codon to facilitate subcloning into the yeast expression vector (pGYR1). A Kozak sequence (marked in italics) was also introduced just upstream of the start codon to achieve high expression of the protein in yeast cells. The PCR products were ligated into pGEM-T (Promega, Madison, WI) using the TA cloning system, and the insert was sequenced in both the forward and reverse directions. The DNA fragment encoding a marmoset CYP2C (tentatively called P450 M-2C) was cut out with *Hin*dIII from the cloned pGEM-T and was subsequently subcloned into pGYR1 digested with the same enzyme. The insert of the plasmid was sequenced to verify the correct orientation with respect to the promoter for pGYR1. Construction of the expression plasmids containing each of CYP2C8, CYP2C9 and CYP2C19 cDNAs was described previously [13].

2.3. Expression of CYP2C enzymes

Saccharomyces cerevisiae AH22 was transformed with pGYR1 containing each of CYP cDNAs by the lithium acetate method, and the cultivation of yeast transformants thus obtained was performed as described [14]. A microsomal fraction was

prepared from yeast cells by the method previously reported [15].

2.4. Assays of M-2C holo- and apoproteins

The microsomal fraction prepared as above was diluted to a protein concentration of 10 mg/ml with 100 mM potassium phosphate buffer (pH 7.4) containing 20% (v/v) glycerol, and the total holo-CYP content was measured spectrophotometrically according to the method of Omura and Sato [16] using 91 mM^{-1} cm^{-1} as the absorption coefficient.

Marmoset liver microsomes were also prepared according to a published method [17]. Appropriate portions of the microsomal fractions of yeast cells, marmoset livers and pooled human livers were subjected to sodium dodecyl sulfate-polyacrylamide gel electrophoresis using a 10% slab gel. Following the electrophosresis, proteins on the gel were electroblotted to a polyvinylidene fluoride membrane, and were analyzed by Western blotting according to the method of Guengerich et al. [18] using rabbit anti-human CYP2C19 polyclonal antibody as a primary antibody (Daiichi Chemical Co.) and peroxidase-goat-anti-rabbit IgG (H + L) as a secondary antibody (Daiichi Chemical Co.).

2.5. Enzyme assay

PT 6α-hydroxylase activity in microsomal fractions from yeast cells expressing P450 M-2C or CYP2C8 was determined by the method of Soyama et al. [19] with a slight modification. Briefly, an ice-cold reaction mixture (500 μl) in a conical glass tube (10 ml) with a stopper contained 5 mM G-6-P, 1 IU of G-6-P dehydrogenase, 5 mM $MgCl_2$, 0.1 mM EDTA, 0.5 mM NADPH and PT (2.5, 5 and 10 μM). After preincubation at 37 °C for 5 min, the reaction was started by adding the microsomal fraction (20 pmol CYP) and was performed at 37 °C for 10 min. After the reaction was stopped by adding 3 ml of ethyl acetate and vortex mixing, 10 nmol of docetaxel was added as an internal standard, and the mixture was shaken at room temperature for 10 min. The mixture was then centrifuged at 1200 × *g* for 15 min, and 2 ml of the organic layer was taken, and evaporated *in vacuo*. The residue was dissolved in 200 μl of methanol/water (1:1, v/v), and an aliquot (10 μl) was subjected to HPLC under the conditions described below.

DF 4′-hydroxylase activity in microsomal fractions from yeast cells expressing M-2C or CYP2C9 was determined by the method of Schmitz et al. [20] with a slight modification. Briefly, a reaction mixture containing the same components described above except for the substrate (5, 20 or 100 μM DF instead of PT) was preincubated at 37 °C for 5 min, and the reaction was started by adding the microsomal fraction (20 pmol CYP) and was stopped 5 min later by adding 20 μl of 2 M phosphoric acid and vortexing. Then, 3 ml of *t*-butylmethylether and 0.8 nmol of *N*-phenylanthranilic acid as an internal standard were added, shaken vigorously, and centrifuged at 1200 × *g* for 15 min. The organic layer (2 ml) was taken, and evaporated *in vacuo*, and the residue was dissolved in 200 μl of methanol/water (1:1, v/v). An aliquot (10 μl) was subjected to HPLC under the conditions described below.

TB *p*-methylhydroxylase activities in microsomal fractions from yeast cells expressing P450 M-2C, CYP2C8, CYP2C9 or CYP2C19 and in pooled human liver microsomes were determined by the method of Komatsu et al. [21] with a slight modification. Briefly, a reaction mixture containing the same components described for PT 6α-hydroxylation except for the substrate (0.25, 1 or 2.5 μM TB instead of PT) was preincubated at 37 °C for 5 min, and the reaction was started by adding the microsomal fraction (20 pmol of recombinant CYP or 1 mg of human liver microsomes) and was stopped 10 min later for the recombinant enzymes and 40 min later for the human liver microsomes by adding 3 ml of ethyl acetate and vortexing. Then, 1.5 μg of chlorpropamide was added as an internal standard, and the mixture was shaken vigorously, and centrifuged at 1200 × *g* for 15 min. The organic layer (2 ml) was taken, and evaporated *in vacuo*, and the residue was dissolved in 200 μl of methanol/water (1:1, v/v). An aliquot (10 μl) was subjected to HPLC under the conditions described below.

S-MP 4′-hydroxylase activity in microsomal fractions from yeast cells expressing P450 M-2C or CYP2C19 was determined by the method of Nakajima et al. [22] with a slight modification. Briefly, a reaction mixture containing the same components described for PT 6α-hydroxylation except for the substrate (10, 50 or 200 μM S-MP instead of PT) was preincubated at 37 °C for 5 min, and the reaction was started by adding the microsomal fraction (20 pmol CYP) and was stopped 5 min later by adding 3 ml of dichloromethane and vortexing. Then 4 nmol of phenobarbital was added as an internal standard, and the mixture was shaken vigorously, and centrifuged at 1200 × *g* for 15 min. The organic layer (2 ml) was taken, and evaporated *in vacuo*, and the residue was dissolved in 200 μl of CH_3OH/water (1:1, v/v). An aliquot (10 μl) was subjected to HPLC under the conditions described below.

The HPLC conditions were: a Hitachi 655A-12 liquid chromatograph equipped with an L-5000 LC controller, a 655A variable wavelength UV monitor, a Rheodyne model 7125 injector and a Shimadzu C-R3A Chromatopac data processor; column, Inertsil ODS 80A (4.6 mm × 150 mm, GL Science Co., Tokyo, Japan) at 40 °C; mobile phase, water/CH_3CN/CH_3OH (52:34:14, v/v) at a flow rate of 1.2 ml/min for PT 6α-hydroxylation (detection, 230 nm), 30 mM potassium phosphate buffer (pH 6.5)/CH_3CN/CH_3OH (64:16:20, v/v) at a flow rate of 1.2 ml/min for DF 4′-hydroxylation (detection, 280 nm), 20 mM potassium phosphate buffer (pH 4)/CH_3CN/CH_3OH (77:6:17, v/v) at a flow rate of 1.0 ml/min for S-MP 4′-hydroxylation (detection, 204 nm), and 0.05% phosphoric acid/CH_3CN (72:28, v/v) at a flow rate of 1.0 ml/min for TB *p*-methylhydroxylation (detection, 230 nm). For each enzyme assay, calibration curves were made by adding various amounts of synthetic metabolites to ice-cold reaction mixtures containing the same components described above. Intra- and inter-day variation coefficients did not exceed 10% in any assay.

2.6. Kinetic and inhibition studies

Kinetic studies for TB *p*-methylhydroxylation were performed using substrate concentration ranges of 0.1–10 mM for P450 M-2C, 0.1–7.5 mM for CYP2C8, 0.025–2.5 mM for CYP2C9 and human liver microsomes, 0.05–5 mM for CYP2C19, and 0.01–5 mM for marmoset liver microsomes. Apparent Michaelis–Menten constants (K_m) and maximal velocities (V_{max}) were

```
   1  ATG GAT CCT TTT GTG GTC CTG TTG CTC TGT CTC TCT TTT TTG CTT CTC TTT TCA CTC TGG   60
   1  Met Asp Pro Phe Val Val Leu Leu Leu Cys Leu Ser Phe Leu Leu Leu Phe Ser Leu Trp   20

  61  AGA CAG AGC TCT GGG AGA GGG AAG CTC CCT CCT GGC CCC ACT CCT CTT CCT ATT ATT GGA  120
  21  Arg Gln Ser Ser Gly Arg Gly Lys Leu Pro Pro Gly Pro Thr Pro Leu Pro Ile Ile Gly   40

 121  AAC ATC CTA CAG ATA AGT GTT AAG GAC ATC GGC AAA TCT TTC AGC AAT CTC TCA AAA GTC  180
  41  Asn Ile Leu Gln Ile Ser Val Lys Asp Ile Gly Lys Ser Phe Ser Asn Leu Ser Lys Val   60

 181  TAT GGT CCT CTG TTC ACC GTG TAT TTT GGC ACG AAG CCC GTA GTG GTG TTG CAC GGA TAT  240
  61  Tyr Gly Pro Leu Phe Thr Val Tyr Phe Gly Thr Lys Pro Val Val Val Leu His Gly Tyr   80

 241  GAG GCA GTA AAG GAA GCC CTG ATT GAT AAT GGA GAG GAG TTT TCT GGA AGA AGC ATT TTC  300
  81  Glu Ala Val Lys Glu Ala Leu Ile Asp Asn Gly Glu Glu Phe Ser Gly Arg Ser Ile Phe  100

 301  CCA GTA TCT CAA AGA ACT TCT AAA GAT CTT GGA ATC ATT TCC AGC AAT GGA AAG AGA TGG  360
 101  Pro Val Ser Gln Arg Thr Ser Lys Asp Leu Gly Ile Ile Ser Ser Asn Gly Lys Arg Trp  120

 361  AAG GAG ATC CGG CGT TTC TCC CTT ACA ACA TTG CGG AAT TTT GGG ATG GGG AAG AGG AGC  420
 121  Lys Glu Ile Arg Arg Phe Ser Leu Thr Thr Leu Arg Asn Phe Gly Met Gly Lys Arg Ser  140

 421  ATT GAG GAC CGT GTT CAA CAA GAA GCC CGC TGC CTT GTG GAG GAG TTG AGA AAA ACC AAG  480
 141  Ile Glu Asp Arg Val Gln Gln Glu Ala Arg Cys Leu Val Glu Glu Leu Arg Lys Thr Lys  160

 481  GCC TCA CCC TGT GAT CCC ACT TTC ATC CTG GGC TGT GCT CCC TGC AAT GTG ATC TGC TCC  540
 161  Ala Ser Pro Cys Asp Pro Thr Phe Ile Leu Gly Cys Ala Pro Cys Asn Val Ile Cys Ser  180

 541  GTT GTT TTC CAG AAT CGA TTT GAT TAT AAA GAT GAA AAT TTT CTC ACC CTG ATG AAA AGG  600
 181  Val Val Phe Gln Asn Arg Phe Asp Tyr Lys Asp Glu Asn Phe Leu Thr Leu Met Lys Arg  200

 601  TTC AAT GAA AAC TTC AAG ATT CTG AGC TCT CCA TGG ATC CAG TTC TGC AAT AAT TTC CCT  660
 201  Phe Asn Glu Asn Phe Lys Ile Leu Ser Ser Pro Trp Ile Gln Phe Cys Asn Asn Phe Pro  220

 661  CTC CTC ATG GAT TAT TTC CCA GGA CCT CAC AAC AAA TTG TTT AAA AAT GTT GCT CTT ACA  720
 221  Leu Leu Met Asp Tyr Phe Pro Gly Pro His Asn Lys Leu Phe Lys Asn Val Ala Leu Thr  240

 721  AAA AGC TAT ATT TGG GAG AAA ATA AAA GAA CAC CAA GCA TCA CTG GAT GTT AAC AAT CCT  780
 241  Lys Ser Tyr Ile Trp Glu Lys Ile Lys Glu His Gln Ala Ser Leu Asp Val Asn Asn Pro  260

 781  CGG GAC TTT ATC GAT TGC TTT CTG ATC AAA ATG CAG CAG GAA AAG GAC AAC CAA GAG TCT  840
 261  Arg Asp Phe Ile Asp Cys Phe Leu Ile Lys Met Gln Gln Glu Lys Asp Asn Gln Glu Ser  280

 841  GAA TTC ACT ATT GAA AGC TTG GTT GGC ACT GTA GCT GAT CTA TTT GTT GCT GGA ACA GAG  900
 281  Glu Phe Thr Ile Glu Ser Leu Val Gly Thr Val Ala Asp Leu Phe Val Ala Gly Thr Glu  300

 901  ACA ACA AGC ACC ACT CTG AGA TAT GGA CTC CTA CTC CTG CTG AAG CAC CCA GAG GTC ACA  960
 301  Thr Thr Ser Thr Thr Leu Arg Tyr Gly Leu Leu Leu Leu Leu Lys His Pro Glu Val Thr  320

 961  GCT AAA GTC CAG GAA GAG ATT GAT CAT GTA ATT GGC AGA CAC AGG AGC CCC TGC ATG CAG 1020
 321  Ala Lys Val Gln Glu Glu Ile Asp His Val Ile Gly Arg His Arg Ser Pro Cys Met Gln  340

1021  GAT AGG AGC CAC ATG CCT TAT ACA GAT GCT GTC ATG CAC GAG ATC CAG AGA TAC ATT GAC 1080
 341  Asp Arg Ser His Met Pro Tyr Thr Asp Ala Val Met His Glu Ile Gln Arg Tyr Ile Asp  360

1081  CTT GTC CCC ACC AGT GTG CCC CAT GCA GTG ACC ACT GAC ATT AAG TTC AGA AAT TAC CTC 1140
 361  Leu Val Pro Thr Ser Val Pro His Ala Val Thr Thr Asp Ile Lys Phe Arg Asn Tyr Leu  380

1141  ATC CCC AAG GGC ACA GCC ATA ATG ACA TCA CTG ACT TCA GTG CTG CAC AGT GAC AAA GAA 1200
 381  Ile Pro Lys Gly Thr Ala Ile Met Thr Ser Leu Thr Ser Val Leu His Ser Asp Lys Glu  400

1201  TTT CCC AAT CCA AAG ACC TTT GAC CCT GGC CAC TTT CTG GAT AAA AAT GGC AAC TTT AAG 1260
 401  Phe Pro Asn Pro Lys Thr Phe Asp Pro Gly His Phe Leu Asp Lys Asn Gly Asn Phe Lys  420

1261  AAA AGT GAC CAC TTC ATG CCT TTC TCA GCA GGG AAA CGA ATT TGT GCT GGA GAG GGA CTC 1320
 421  Lys Ser Asp His Phe Met Pro Phe Ser Ala Gly Lys Arg Ile Cys Ala Gly Glu Gly Leu  440

1321  GCC CGC ATG GAG ATA TTT TTA TTC CTA ACC ACA ATT TTA CAG AAC TTT AAT CTG AAA TCT 1380
 441  Ala Arg Met Glu Ile Phe Leu Phe Leu Thr Thr Ile Leu Gln Asn Phe Asn Leu Lys Ser  460

1381  GTT GGC GAT ATA AAG AAC CTC AAT ACT ACT TCA GCT AGC AAA TCA ATT GTT TCT TTG CCA 1440
 461  Val Gly Asp Ile Lys Asn Leu Asn Thr Thr Ser Ala Ser Lys Ser Ile Val Ser Leu Pro  480

1441  CCC CCG TAC CAG ATC TGC TTC ATT CCT GTC TGA  1473
 481  Pro Pro Tyr Gln Ile Cys Phe Ile Pro Val End
```

Fig. 1 – Nucleotide and deduced amino acid sequences of marmoset P450 M-2C. The numbers of the amino acids and nucleotides are shown in upper and lower lines, respectively.

```
M-2C        1  MDPFVVLLLCLSFLLLFSLWRQSSGRGKLPPGPTPLPIIGNILQISVKDIGKSFSNLSKV  60
CYP2C8      1  MEPFVVLVLCLSFMLLFSLWRQSCRRRKLPPGPTPLPIIGNMLQIDVKDICKSFTNFSKV  60
CYP2C9      1  MDSLVVLVLCLSCLLLLSLWRQSSGRGKLPPGPTPLPVIGNILQIGIKDISKSLTNLSKV  60
CYP2C19    61  MDPFVVLVLCLSCLLLLSIWRQSSGRGKLPPGPTPLPVIGNILQIDIKDVSKSLTNLSKI  60
               *   *** ****  ** * ****  * ********** *** ***  **  **  * **

                                                          SRS-1
M-2C       61  YGPLFTVYFGTKPVVVLHGYEAVKEALIDNGEEFSGRSIFPVSQRTSKDLGIISSNGKRW  120
CYP2C8     61  YGPVFTVYFGMNPIVVFHGYEAVKEALIDNGEEFSGRGNSPISQRITKGLGIISSNGKRW  120
CYP2C9     61  YGPVFTLYFGLKPIVVLHGYEAVKEALIDLGEEFSGRGIFPLAERANRGFGIVFSNGKKW  120
CYP2C19    61  YGPVFTLYFGLERMVVLHGYEVVKEALIDLGEEFSGRGHFPLAERANRGFGIVFSNGKRW  120
               *** ** ***    ** **** ******* *******   *   *     **  **** *

M-2C      121  KEIRRFSLTTLRNFGMGKRSIEDRVQQEARCLVEELRKTKASPCDPTFILGCAPCNVICS  180
CYP2C8    121  KEIRRFSLTNLRNFGMGKRSIEDRVQEEAHCLVEELRKTKASPCDPTFILGCAPCNVICS  180
CYP2C9    121  KEIRRFSLMTLRNFGMGKRSIEDRVQEEARCLVEELRKTKASPCDPTFILGCAPCNVICS  180
CYP2C19   121  KEIRRFSLMTLRNFGMGKRSIEDRVQEEARCLVEELRKTKASPCDPTFILGCAPCNVICS  180
               ********  ***************** ** ****************************

                         SRS-2                                  SRS-3
M-2C      181  VVFQNRFDYKDENFLTLMKRFNENFKILSSPWIQFCNNFPLLMDYFPGPHNKLFKNVALT  240
CYP2C8    181  VVFQKRFDYKDQNFLTLMKRFNENFRILNSPWIQVCNNFPLLIDCFPGTHNKVLKNVALT  240
CYP2C9    181  IIFHKRFDYKDQQFLNLMEKLNENIKILSSPWIQICNNFSPIIDYFPGTHNKLLKNVAFM  240
CYP2C19   181  IIFQKRFDYKDQQFLNLMEKLNENIRIVSTPWIQICNNFPTIIDYFPGTHNKLLKNLAFM  240
                 *  ******  ** **   ***  *   **** ****    * *** ***  ** *

                                                          SRS-4
M-2C      241  KSYIWEKIKEHQASLDVNNPRDFIDCFLIKMQQEKDNQESEFTIESLVGTVADLFVAGTE  300
CYP2C8    241  RSYIREKVKEHQASLDVNNPRDFMDCFLIKMEQEKDNQKSEFNIENLVGTVADLFVAGTE  300
CYP2C9    241  KSYILEKVKEHQESMDMNNPQDFIDCFLMKMEKEKHNQPSEFTIESLENTAVDLFGAGTE  300
CYP2C19   241  ESDILEKVKEHQESMDINNPRDFIDCFLIKMEKEKQNQQSEFTIENLVITAADLLGAGTE  300
                * * ** **** * * *** ** **** **  ** ** *** ** *  *  **  ****

          ------                                                        ---
M-2C      301  TTSTTLRYGLLLLLKHPEVTAKVQEEIDHVIGRHRSPCMQDRSHMPYTDAVMHEIQRYID  360
CYP2C8    301  TTSTTLRYGLLLLLKHPEVTAKVQEEIDHVIGRHRSPCMQDRSHMPYTDAVVHEIQRYSD  360
CYP2C9    301  TTSTTLRYALLLLLKHPEVTAKVQEEIERVIGRNRSPCMQDRSHMPYTDAVVHEVQRYID  360
CYP2C19   301  TTSTTLRYALLLLLKHPEVTAKVQEEIERVIGRNRSPCMQDRGHMPYTDAVVHEVQRYID  360
               ******** ******************  **** ******** ******** ** *** *
          SRS-5
M-2C      361  LVPTSVPHAVTTDIKFRNYLIPKGTAIMTSLTSVLHSDKEFPNPKTFDPGHFLDKNGNFK  420
CYP2C8    361  LVPTGVPHAVTTDTKFRNYLIPKGTTIMALLTSVLHDDKEFPNPNIFDPGHFLDKNGNFK  420
CYP2C9    361  LLPTSLPHAVTCDIKFRNYLIPKGTTILISLTSVLHDNKEFPNPEMFDPHHFLDEGGNFK  420
CYP2C19   361  LIPTSLPHAVTCDVKFRNYLIPKGTTILTSLTSVLHDNKEFPNPEMFDPRHFLDEGGNFK  420
               * **  ***** * *********** *   ******  ******  *** ****  ****

                                                          SRS-6
M-2C      421  KSDHFMPFSAGKRICAGEGLARMEIFLFLTTILQNFNLKSVGDIKNLNTTSASKSIVSLP  480
CYP2C8    421  KSDYFMPFSAGKRICAGEGLARMELFLFLTTILQNFNLKSVDDLKNLNTTAVTKGIVSLP  480
CYP2C9    421  KSKYFMPFSAGKRICVGEALAGMELFLFLTSILQNFNLKSLVDPKNLDTTPVVNGFASVP  480
CYP2C19   421  KSNYFMPFSAGKRICVGEGLARMELFLFLTFILQNFNLKSLIDPKDLDTTPVVNGFASVP  480
               **  *********** ** ** ** ***** *********  * * * **       * *

M-2C      481  PPYQICFIPV  491
CYP2C8    481  PSYQICFIPV  491
CYP2C9    481  PFYQLCFIPV  491
CYP2C19   481  PFYQLCFIPV  491
               * ** *****
```

Fig. 2 – Multiple alignment of the amino acid sequences of P450 M-2C, human CYP2C8, CYP2C9 and CYP2C19. *Amino acid residues conserved among the four CYP2C enzymes. Six substrate recognition sites (SRSs) are shown with lines.

analyzed on the basis of Michaelis–Menten plots or Eadie–Hofstee plots using Prism Version 4 (Graphpad Software, San Diego, CA). Inhibition experiments using quercetin (10, 50 and 200 μM), sulfaphenazole (20, 50 and 200 μM) and omeprazole (50, 200 and 500 μM) and substrate (TB) concentrations of 0.1 and 1 mM were performed for marmoset liver microsomes and yeast cell microsomes expressing P450 M-2C. Each inhibitor was dissolved in a mixture of methanol/dimethylsulfoxide (1:1, v/v) and the final concentration of the organic solvent in the reaction mixture was less than 1%. Control experiments were run with the vehicle only instead of the inhibitors. IC_{50} values were analyzed using Prism. Protein concentrations were measured by the method of Lowry et al. [23] using bovine plasma albumin as a standard.

2.7. *Molecular modeling*

The homology model of P450 M-2C was constructed by Swiss-Model (http://swissmodel.expasy.org/) using the crystallo-

Table 1 – Identities of the nucleotide and deduced amino acid sequences of eight CYP2C enzymes in primates

	M-2C	CYP2C8	CYP2C9	CYP2C19	CYP2C20	CYP2C43	CYP2C74	CYP2C75
M-2C		92.7	84.5	83.8	93.1	83.3	93.1	83.6
CYP2C8	87.1		84.7	84.9	95.6	83.8	95.5	84.5
CYP2C9	78.4	77.6		94.8	84.5	95.2	84.5	95.9
CYP2C19	77.1	77.8	91.4		84.7	93.8	84.6	94.8
CYP2C20	88.8	91.6	78.2	78.6		83.2	99.6	84.3
CYP2C43	76.7	77.1	92.2	90.0	77.1		83.1	95.1
CYP2C74	89.0	91.6	78.2	78.4	99.4	76.9		84.2
CYP2C75	76.5	76.7	93.9	92.0	77.1	93.5	76.9	

Upper-right values, percentage identities of the nucleotide sequences; lower-left values, percentage identities of deduced amino acid sequences.

graphic data of CYP2C8 (1PQ2) obtained from Protein Data Bank (http://www.rcsb.org/pdb/) and the primary amino acid sequence of P450 M-2C determined in this work. Hydrogen atoms were further added for the P450 M-2C homology model using the Biopolymer module of Insight II software package (Molecular Simulations Inc., San Diego, CA). Six peptides of P450 M-2C (Arg-97 to Asn-116, Met-198 to Ser-209, Phe-234 to Leu-239, Gly-289 to Ser-303, Ile-359 to His-368, and Thr-469 to Ser-478) were extracted as substrate recognition sites (SRSs). The active-site cavities of CYP2C8 and P450 M-2C were made manually above the sixth ligand of heme at 1.0 Å resolution using a homemade CG program working on Windows PC. The amino acid residues at the active sites of CYP2C8 and P450 M-2C were drawn using RasMol Version 2.6-ucb-1.0 as described elsewhere [24].

3. Results

3.1. *Sequence analysis*

As shown in Fig. 1, the cloned cDNA consisted of 1473 base pairs starting with an initiation codon ATG and ending with a termination codon TGA. Fig. 2 depicts a comparison of deduced amino acid sequences of P450 M-2C, human CYP2C8, CYP2C9 and CYP2C19. The nucleotide and amino acid sequences are compared with those of human and monkey P450s belonging to the CYP2C subfamily in Table 1. The nucleotide sequence of the cDNA encoding marmoset P450 M-2C showed 92.7, 84.5, 83.8, 93.1, 83.3, 93.1 and 83.6% identities to human CYP2C8 (GenBank accession no. NM-000770), CYP2C9 (NM-000771), CYP2C19 (NM-000769), crab-eating mon-

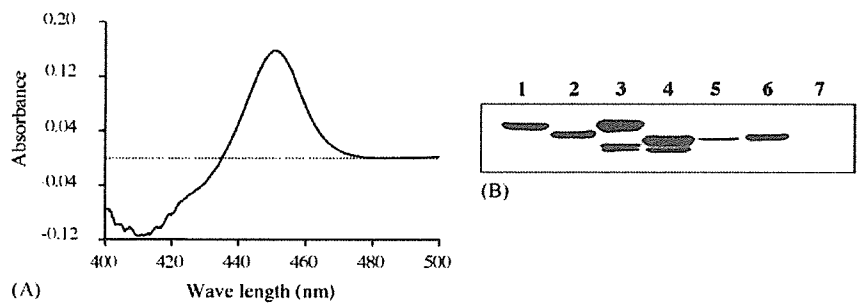

Fig. 3 – A reduced CO-difference spectrum of yeast cell microsomes expressing marmoset P450 M-2C (A) and Western blot analysis of microsomal fractions from human and marmoset livers and of yeast cells expressing P450 M-2C and human CYP2C enzymes (B). (A) The protein concentration used was 10 mg/ml. (B) Lane 1, human liver microsomes; lane 2, yeast cell microsomes expressing human CYP2C8; lane 3, yeast cell microsomes expressing human CYP2C9; lane 4, yeast cell microsomes expressing human CYP2C19; lane 5, yeast cell microsomes expressing marmoset P450 M-2C; lane 6, marmoset liver microsomes; lane 7, mock. The amounts of microsomal proteins used were 30 μg for human and marmoset livers and 15 μg for yeast cells expressing P450 M-2C and human CYP2C enzymes.